Université de Montréal

Search for Heavy Leptons with the OPAL Detector

par
Erik Elfgren
Département de physique
Faculté des arts et des sciences

Mémoire présenté à la Faculté des études supérieures
en vue de l'obtention du grade de
Maître ès sciences (M.Sc.)
en physique

Avril, 2002

©Erik Elfgren, 2002

Université de Montréal
Faculté des études supérieures

Ce mémoire intitulé:

Search for Heavy Leptons with the OPAL Detector

présenté par:

Erik Elfgren

a été évalué par un jury composé des personnes suivantes:

Paul Taras,	président-rapporteur
Georges Azuelos,	directeur de recherche
David London,	membre du jury

Mémoire accepté le: .....

SOMMAIRE

Ce mémoire de Maîtrise a pour object une recherche de leptons exotiques. Cette recherche a été effectuée à l'aide des données enregistrées par le detécteur OPAL utilisant les collisions e^+e^- produites au sein de l'accélérateur LEP "Large Electron Positron collider" au CERN. L'énergie dans le centre de masse etait dans l'intervalle 183-209 GeV et la luminosité integrée était de 663 pb^{-1}. Le processus étudié est la production de leptons lourds par la voie du courant chargé suivi de la désintégration du W en deux quarks. En particulier, on s'est penché sur la production simple de leptons lourds dans la région de masse 100-170 GeV. Aucune évidence de l'existence d'une nouvelle particule n'a été trouvée. Toutefois, les résultats de cette analyse imposent des limites supérieures sur le mélange entre un lepton lourd et le lepton ordinaire pour différentes masses du lepton lourd. Les limites sur ces angles de mélange sont généralement meilleures que la valeur nominale $\zeta^2 \sim 0.005$.

Mots clés : physique, particules, OPAL, leptons exotiques, leptons lourds, leptons excités, detection.

Abstract

This M.Sc. thesis describes a search for exotic leptons. The search has been performed using data from the OPAL detector at the Large Electron Positron collider at CERN. The total integrated luminosity was 663 pb^{-1} with center of mass energies in the range of 183-209 GeV. The work has been concentrated on the study of production of heavy leptons via the charged current channel and disintegration of the W into two quarks. In particular, single production of heavy leptons in the mass region 100-170 GeV has been extensively studied. No evidence for any new particles has been found. The results translate into upper limits on the mixing between the heavy and the ordinary lepton for different heavy lepton masses. The limits on the mixing angles are generally improved in comparison with the nominal value $\zeta^2 \sim 0.005$.

Key words : physics, particles, OPAL, exotic leptons, heavy leptons, excited leptons.

Preface

This Master of Science project has been carried out at Université de Montréal under the supervision of Georges Azuelos. The research has been done within the framework of the OPAL collaboration.

Regarding the notations used, a capital letter in fermion names signifies a heavy fermion (e. g. L=heavy lepton, E=heavy electron) while a star signifies an excited fermion (e. g. u^*=excited up-quark, μ^*=excited muon). A fermion is either a lepton or a quark, and an exotic particle is either heavy or excited. A $\pm$ denotes a charged fermion (e. g. $L^{\pm}$=charged heavy lepton) and a neutral lepton is synonymous to a neutrino. A lepton L can be either charged or neutral. A bar denotes an anti-particle. Unless otherwise specified, $c = \hbar = 1$. For further details on symbols, constants, and abbreviations, see Appendix B. In the text, footnotes are used to explain something in more detail, and they are not needed for the basic comprehension. Words which appear *slanted* are explained in the Glossary in Appendix A.

I would also like to thank all the people who have helped me. First of all, my supervisor Georges Azuelos who has always taken the time to answer my questions properly and has given me a hand whenever I have had difficulties. He has given me a lot of liberty, but also a great support. I would also like to thank Robert McPherson who has been of great help in the simulations and has shared his general reflections on the problem. Finally, thanks to David London, Richard Teuscher and Alain Bellerive for valuable discussions, and to Réda Tafirout for his preliminary work on the subject.
Montréal, May 2002.

Erik Elfgren

Table of Contents

Abstract **i**

Preface **ii**

Table of Contents **iii**

List of Tables **vii**

List of Figures **x**

Chapter 1: Introduction **1**

1.1 Background 1

1.2 Outline of Thesis 4

1.3 Excited Fermions 5

1.4 Heavy Fermions 6

1.5 Present Contraints 8

1.5.1 Mixing 10

1.6 The Detector 11

1.6.1 The LEP Accelerator 11

1.6.2 The OPAL Detector 11

Chapter 2: Phenomenology **16**

2.1 Introduction 16

2.2 General 16

2.2.1 Comments About Cross Section Generation 18

2.3 Double Production of Exotic Leptons 19

2.4 Single Production of Exotic Leptons 20

2.4.1 Branching Ratio $\Gamma_{CC/NC}$ 23

2.4.2 Heavy Leptons 24

2.4.3 Excited Leptons 26

Chapter 3: Simulation and Selection **28**

3.1 Introduction 28

3.2 Signal Generation 29

3.2.1 General 30

3.2.2 Heavy Leptons 31

3.2.3 Excited Leptons 32

3.3 Backgrounds 32

3.4 Variables and Cuts 35

3.4.1 Description of Variables 35

3.4.2 Preliminary Cuts 37

3.5 Complete Analysis of Heavy Neutrinos 38

3.5.1 Cuts 40

3.6 Discussion of Heavy Charged Leptons 44

Chapter 4: Data Analysis and Results **50**

4.1 Heavy Neutral Lepton 50

4.1.1 Lower Limits on the Mixing 53

4.1.2 Upper Mixing Limits 54

4.1.3 Systematic Errors 57

Chapter 5: Conclusions and Outlook **61**

5.1 Conclusions 61

5.2 Outlook 61

Appendix A: Glossary **63**

Appendix B: List of Symbols **66**

B.1 Exotic Particles 67

B.2 Standard Model Particles 68

B.3 Variables 69

B.4 List of Constants 69

B.5 Abbreviations 70

Bibliography **71**

List of Tables

1-I The three families/generations of leptons (electrons, e, and electron neutrinos, ν_e; muons, μ, and muon neutrinos, ν_μ; taus, τ, and tau neutrinos, ν_τ) and quarks (up, u; down, d; charm, c; strange, s; top, t; and bottom, b) . The quarks d', s', b' are the weakly interacting mixed states of the mass eigenstates d, s, b. The indices L and R refer to left and right handed particles (for left-handed particles the spin is antiparallel with the direction of the particle, the spin points "backwards"). . . . 2

2-I Cross sections, σ_j (pb) for single heavy neutrino production for different masses, M_N (GeV) and center of mass energies, $\sqrt{\hat{s}}$ (GeV). 26

3-I Integrated luminosities at LEP for different center of mass energies. The total integrated luminosity, $\Sigma \int \mathcal{L} dt = 663.5$ pb^{-1}. The energies in the center of mass system are approximate within 1-2 GeV. 28

3-II Background processes. The $\gamma^* \gamma qq$ background has 150k events for E=183, 189, 196 and 200 GeV; 350k events for E=192, 202, 204, 205, 207, 208 GeV and 330k events for E=206 GeV. 34

3-III Cross sections for background processes for different energies. Energy given in GeV. There are no simulations for $203, 209$ GeV, but their luminosities are so low that it does not matter. 34

3-IV The effect of the preliminary cuts. The reduction is defined as the number of events before divided by the number of events after the preliminary cuts. 38

3-V Summary of cuts for the different masses M_N for the energy region 180-190 GeV. Energies and masses are given in GeV, angles in radians. For explanations of variables, see section 3.4.1Description of Variablessubsection.3.4.1. For readability, 2.5 and 7.5 are displayed as 3 and 8, respectively. 44

3-VI Summary of cuts for the different masses M_N for the energy region 191-200 GeV. Energies and masses are given in GeV, angles in radians. 44

3-VIISummary of cuts for the different masses M_N for the energy region 201-210 GeV. Energies and masses are given in GeV, angles in radians. 45

3-VIINumber of remaining events for different backgrounds before each cut for $M_N = 100$ GeV in the energy region 191-200 GeV. 45

3-IX Number of remaining events for different backgrounds before each cut for $M_N = 170$ GeV in the energy region 191-200 GeV. 48

4-I Number of remaining events before each cut for $M_N = 100$ GeV in the energy region 191-200 GeV. 52

4-II Number of remaining events before each cut for $M_N = 170$ GeV in the energy region 191-200 GeV. 53

4-III Upper limits on the mixing parameter, ζ^2, with 95% CL, for different masses and in the energy region 180-190 GeV. Note that the values given for the mixing parameter have to be divided by 1000. 55

4-IV Upper limits on the mixing parameter, ζ^2, with 95% CL, for different masses and in the energy region 191-200 GeV. Note that the values given for the mixing parameter have to be divided by 1000. 55

4-V Upper limits on the mixing parameter, ζ^2, with 95% CL, for different masses and in the energy region 201-208 GeV. Note that the values given for the mixing parameter have to be divided by 1000. 56

4-VI Combined upper limits on the mixing parameter for different masses for the the three energy regions. The nominal value of the mixing parameter is $\zeta^2 = 0.005$. 56

4-VII Effect on the results for changes in cuts for $M_N = 100$ GeV in the center of mass energy region 191-200 GeV 59

4-VIII Effect on the results for changes in cuts for $M_N = 170$ GeV in the center of mass energy region 191-200 GeV. 60

List of Figures

1-1 The mass hierarchy of the three fermion generations 3

1-2 Mixing,ζ^2, between an ordinary and a heavy lepton. 10

1-3 The OPAL detector 12

2-1 s-channel single production processes for heavy/excited fermions. (a) Charged exotic (heavy or excited) lepton, L^*. (b) Neutral exotic lepton, N^*. . 17

2-2 s-channel double production processes for heavy/excited fermions. (a) Charged exotic leptons, L^*. (b) Neutral exotic leptons, N^*. 19

2-3 Cross sections for double production of different types of exotic leptons at $E_{CMS} = 207$ GeV. All the types of heavy charged leptons, L, have the same cross section σ_L and all the types of heavy neutral leptons, N, have the same cross section σ_N. The different types of heavy leptons are discribed in section 1.4Heavy Fermionssection.1.4. The heavy lepton case assumes a mixing angle $\zeta^2 = 0.005$. The excited lepton case assumes a mass scale $\Lambda^2 = 1$ TeV and $f = f' = 1$ (see section 2.4.3Excited Leptonssubsection.2.4.3). problems. 21

2-4 t-channel single production processes for heavy/excited fermions. (a) Charged exotic lepton, L^*. (b) Neutral exotic lepton, N^*. 22

2-5 Cross sections for single production of different types of exotic leptons at $E_{CMS} = 200$ GeV. All the different types of heavy leptons (as described in section 1.4Heavy Fermionssection.1.4) have the same cross section. The heavy lepton case supposes a mixing angle $\zeta^2 = 0.005$. . 23

2-6 Cross sections for single production of different types of exotic leptons as a function of energy. All the types of heavy leptons have the same cross section. The heavy lepton case supposes a mixing angle $\zeta^2 = 0.005$. 24

2-7 Branching ratio $L \to W/Z + \ell$ for single production of heavy leptons as a function of energy. All the types of heavy leptons, charged as well as neutral, have the same branching ratio. 25

3-1 Comparison of the principal variables for different backgrounds. The integrated luminosity $\int \mathcal{L} dt = 79.3$ pb^{-1} and the center of mass energy $E_{CMS} = 200$ GeV. 39

3-2 Comparison of reconstructed masses M_L and M_N for different backgrounds 40

3-3 Comparison of variables relevant for exotic neutral lepton production for different backgrounds 41

3-4 Cuts for $M_N = 100$ GeV in the energy region 191-200 GeV. The background (dotted lines) has been plotted for comparison. Data (stars) have been plotted for reference but have not been used in any way during the optimization. 46

3-5 Cuts for $M_N = 170$ GeV in the energy region 191-200 GeV. The background (dotted lines) has been plotted for comparison. Data (stars) have been plotted for reference but have not been used in any way during the optimization. 47

3-6 When the primary lepton moves very close to the beam pipe, it escapes detection and is confounded with the neutrino. 48

3-7 Energies of detected recoil leptons for M_L =90, 100, 120, 150 GeV. . . 49

3-8 Pre-detector evaluation of signals. Reconstructed heavy charged lepton (L) mass for M =90, 100, 120, 150 GeV. The corresponding heavy neutral lepton (N) reconstructed mass in included for reference (dotted lines). We note that the lower energy has a very bad resolution in the charged lepton case. 49

4-1 Illustration of the statistic distribution 51

Chapter 1

Introduction

1.1 Background

Ever since the discovery of the three families/generations of light leptons and quarks striking similarites have intrigued physicists:

- Similarity between families.
- Similar group structure of leptons and quarks
- Mass hierarchy
- Equal charge

The Standard Model of particle physics [1] postulates three families of leptons and quarks. However, there is no underlying theory predicting these families to be three or predicting the number to be the same for leptons and for quarks.[1] So far, it is only an experimental fact. Thus, a priori, there is no reason why this number should be restricted to three only. In fact, the situation is rather the opposite: there is theoretical justification for *more* than three generations of leptons/quarks (cf. section 1.4).

[1] In fact, in order for the Standard Model to be anomaly-free, the sum of the charge of all fermions must be zero, though this does not necessarily imply an equal number of leptons and quarks.

Within the lepton family there is nothing to distinguish an electron from a muon or a tau, except its mass (and its lepton number). Furthermore, the symmetry of the group structure of leptons and quarks (cf. table 1-I) is a remarkable coincidence. In the

Leptons:	$\begin{pmatrix} \nu_e \\ e \end{pmatrix}_L, \; e_R$	$\begin{pmatrix} \nu_\mu \\ \mu \end{pmatrix}_L, \; \mu_R$	$\begin{pmatrix} \nu_\tau \\ \tau \end{pmatrix}_L, \; \tau_R$
Quarks:	$\begin{pmatrix} u \\ d' \end{pmatrix}_L, \; u_R, d_R$	$\begin{pmatrix} c \\ s' \end{pmatrix}_L, \; c_R, s_R$	$\begin{pmatrix} t \\ b' \end{pmatrix}_L, \; t_R, b_R$

Table 1-I: The three families/generations of leptons (electrons, e, and electron neutrinos, ν_e; muons, μ, and muon neutrinos, ν_μ; taus, τ, and tau neutrinos, ν_τ) and quarks (up, u; down, d; charm, c; strange, s; top, t; and bottom, b) . The quarks d', s', b' are the weakly interacting mixed states of the mass eigenstates d, s, b. The indices L and R refer to left and right handed particles (for left-handed particles the spin is antiparallel with the direction of the particle, the spin points "backwards").

past, symmetries of this kind have been recognized as a sign of substructure. Also the remarkable mass distribution in figure 1-1 is an argument for either a substructure of fermions or for a classification as a representation of a larger group. If a substructure exists, then excited states ought to exist. If there is a larger group it might very well contain heavy leptons. A priori, there is no relation between heavy and excited leptons.

The hierarchy of the masses suggests the possibility of a fourth, even heavier, generation of leptons. Its mass would be of the order of 100 GeV, which could be within the reach of the LEP accelerator where the sensitivity reaches up to $M \sim 200$ GeV in single production and up to $M \sim 100$ GeV in double production. The corresponding neutrino mass would, in principle, also have to be large ($\gtrsim M_Z/2$) in order to be in accord with the measured invisible width of the Z (see section 1.5).

Besides the arguments in favor of heavy and excited fermions there are also several problems with the Standard Model.

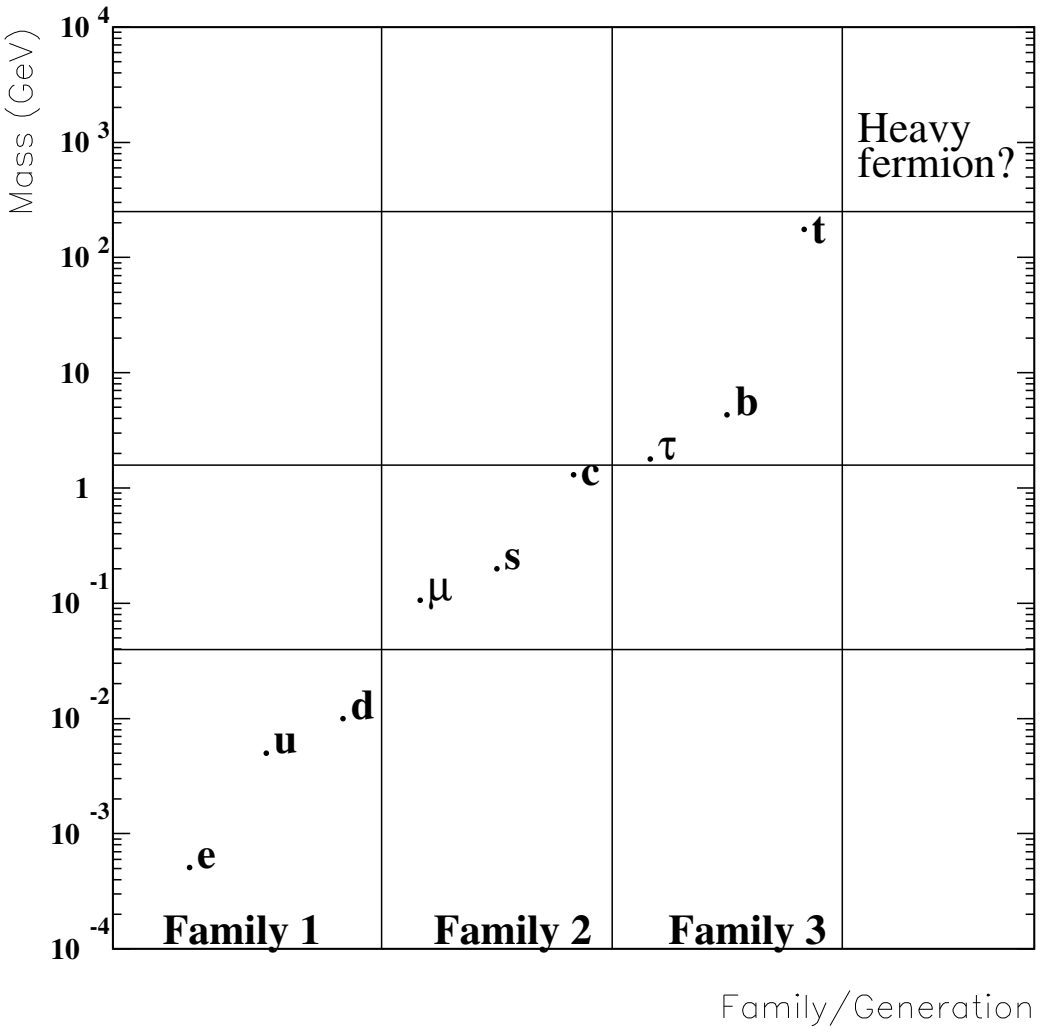

Figure 1-1: The mass hierarchy of the three fermion generations

1. The Standard Model has more than 20 **free parameters** which have to be determined experimentally (three lepton masses, six quark masses, W^+, W^-, Z^0 and Higgs boson masses, three coupling constants, four quark mixing angles, in addition to the masses and mixing angles of the neutrinos).

2. The form of the **Higgs** potential is somewhat arbitrary. The *Higgs particle* has not yet been found and the stability of its mass against radiative corrections is fine-tuned.

3. The nature and origin of the **CP violation** is introduced ad hoc as a complex phase in the CKM matrix.

1.2 Outline of Thesis

This thesis is divided into five chapters. The introduction offers some reasons for the interest in the subject of exotic leptons, as well as it presents a theoretical introduction to the subject, and a summary of the results of previous research. A brief description of the OPAL detector is also given. After that the phenomenology of excited and heavy leptons is presented in chapter 2. The word phenomenology refers to the characteristics of the exotic leptons, which can be used to distinguish them from the background noise of ordinary particles. The following chapter describes the simulations, both of the signal and of the background. In this chapter, the process of event selection is also discussed. This process is concentrated on the single production of heavy leptons, which is the main issue of this thesis. Chapter four describes the data analysis itself with the results in the form of confidence limits on the masses and *mixing parameter* involved in the theory. The conclusion in chapter 5 offers a summary of the results, an outlook of what remains to be done, and possibilities of improvement.

Below are presented some theoretical features of excited and heavy leptons. However, this thesis will not dwell long on the theoretical properties of different models, but rather will investigate their phenomenology and the parameters of importance to detection. This will be the subject of Chapter 2. So far, these theories are not (yet) supported by any experimental evidence.

1.3 Excited Fermions

If a particle has an excited state, this means that it also has a substructure. The excitation is nothing else than a rearrangement of the internal structure, just like an atom or a molecule rearranges its constituents when (de)exciting. Excitation means stored potential energy, just like that in a waterfall.

In the literature [2], the constituents of excited fermions are called *preons*. Different models have been proposed; the number of preons is usually, rather arbitrarily, set to two or three, where the three preon case can have two of them bound together in a bosonic state (see e. g. [3]).

Here are a few arguments in favour of the existence of excited leptons:

- There are unstable and mixed leptons and quarks, and neutrinos are oscillating [4]. From a philosophical viewpoint, these are not desirable properties for a fundamental particle. In the past, these effects have also been shown to be signs of substructure (e. g. atomic and hadronic decays, Kaon oscillation etc.).
- In some preon models [3] the masses of the Z^0 and $W^\pm$ can be explained without the introduction of a Higgs boson. The Z^0 and $W^\pm$ are considered to be preon-antipreon states in analogy with the strong force that can be said to be mediated by quark-antiquark pairs (mesons). This would certainly be of interest if the Higgs particle is not found in the next generation of accelerators.

The catch with the preon models is that they must be able to reproduce *all* experimental data with the new configuration and properties of the preons. This is already the case for e. g. the Supersymmetry and the Grand Unified Theory models, since they are extensions of the Standard Model. However, *new* particles have to be shown to reproduce current data. Even though there remain several theoretical

problems within current preon models they still have many attractive features as mentioned in the previous paragraph.

In this thesis, the detailed description of a specific model is not important, as we study the phenomenological properties of excited leptons from a general point of view.

1.4 Heavy Fermions

Several theories predict the existence of new, heavy fermions. These extensions of the Standard Model generally have a mass scale at which a certain symmetry is restored. If we can obtain accelerator energies reaching this mass scale, we can directly probe the validity of the theory. However, these energies are generally far too high ($M \sim 10^{12}$ TeV) to be reached for our present accelerators ($E \sim 1$ TeV).

The most ambitious of the theories is the Superstring Theory ($M \sim 10^{16}$ TeV), aiming at unifying all the known forces: electromagnetic. weak, strong and gravitational. It is currently the only viable theory to do so. The Grand Unified Theories (unifications at $M \sim 10^{15}$ TeV) attempt all the above, except that they do not include gravity. Supersymmetry Theory, which basically is a way of explaining the mass hierarchy discussed above, is an integral part of both the Superstring Theory and most of the Grand Unified Theories.

A characteristic property of these extended models is that they predict a zoo of new particles, which have to be detected in order to be validated. The experimental advantage is that they offer some concrete predictions to search for.

The Grand Unified groups have fermion representations which contain the Standard Model quarks and leptons but often also additional fermions. The wide range of

masses of the fermions suggests that some new leptons could have masses of about 100 GeV, which is within reach of LEP.

There are three popular unifying groups $SU(5)$, $SO(10)$, and E_6, the latter two contain new fermions. The group $SO(10)$ [5] contains a right-handed Majorana neutrino and it is one of the simplest groups in which the Standard Model could be conveniently embedded ($SU(5)$ is the simplest). The exceptional group E6 [6] contains several singlet neutrinos as well as new charged leptons and quarks and it is an acceptable four-dimensional field theoretical limit of Super String Theory,

There are four phenomenologically different types of heavy leptons (compare with table 1-I):

- **Sequential**

  A fourth generation of fermions with the same basic properties as the other three.

  $$\begin{pmatrix} N \\ L^{\pm} \end{pmatrix}_L ; \; L_R^{\pm}$$

  $$\begin{pmatrix} U \\ D \end{pmatrix}_L ; \; U_R, D_R$$

- **Mirror**

  Doublets have right chirality and singlets have left (opposite of the Standard Model).

  $$\begin{pmatrix} N \\ L^{\pm} \end{pmatrix}_R ; \; L_L^{\pm}$$

  $$\begin{pmatrix} U \\ D \end{pmatrix}_R ; \; U_L, D_L$$

  Mirror fermions occur in many extensions of the Standard Model trying to restore the left-right symmetry [7] at the scale of the electroweak symmetry breaking.

- **Vectorial**

  Both the right and left chirality are doublets.

  $$\begin{pmatrix} N \\ L^{\pm} \end{pmatrix}_L ; \begin{pmatrix} N \\ L^{\pm} \end{pmatrix}_R$$

  $$\begin{pmatrix} U \\ D \end{pmatrix}_L ; \begin{pmatrix} U \\ D \end{pmatrix}_R$$

  Vector fermions occur e. g. in the group E_6.

- **Singlet**

  Both the right and left chirality are singlets.

  $L_L^{\pm},\ L_R^{\pm}\ ;\ N_L,\ N_R$

  $U_L,\ D_R\ ;\ U_R,\ D_L$

  Singlet fermions are found both in E_6 and in $SO(10)$.

In this thesis the focus will be on sequential heavy leptons, also called fourth generation leptons. These new leptons are of the same character as the ones already known.

An experimental reason for searching for this type of leptons is the recent evidence for the mass of neutrinos [8]. The see-saw mechanism [9] can be used to generate massive neutrinos. The mechanism predicts new neutrinos with masses, which could be reachable at LEP.

1.5 Present Contraints

In this section, the present experimental limits in the search for exotic (i. e. heavy and excited) fermions and in particular, for exotic leptons, are outlined. In the past, several searches have been performed in order to find traces of excited and heavy leptons.

Lower limits on the masses of heavy leptons were obtained in e^+e^- collisions at centre-of-mass energies, $\sqrt{s}$, around M_Z [10], and recent searches at $\sqrt{s}$ = 130-140 GeV [11, 12], $\sqrt{s}$ = 161 GeV [13, 14], $\sqrt{s}$ = 172 GeV [14, 15], $\sqrt{s}$ = 130-183 GeV [16, 17, 18], and $\sqrt{s}$ = 200-209 GeV [19] have improved these limits. Excited leptons have been sought at $\sqrt{s} \sim M_Z$ [20], $\sqrt{s}$ = 130-140 GeV [21, 22], $\sqrt{s}$ = 161 GeV [23, 24], $\sqrt{s}$ = 172 GeV [15], $\sqrt{s}$ = 183 GeV [18, 17], $\sqrt{s}$ = 189 GeV [25], and at the HERA ep collider [26]. If direct production is kinematically forbidden, the cross-sections of processes such as $e^+e^- \to \gamma\gamma$ and $e^+e^- \to f\bar{f}$ [27, 28] are sensitive to new particles at higher masses through loop corrections.

For double production of heavy leptons, masses up to 103 GeV have been explored [19]. For single production of heavy leptons, this thesis covers masses up to 170 GeV. In both cases it is the charged current channel that has been studied because it has higher branching ratio than the neutral current channel.

For single production of excited leptons in all important decay modes, the most recent results are found in [29] where all LEP data are combined.

Most searches for new particles, predicted by models beyond the Standard Model, assume that the new particles decay promptly at the primary interaction vertex due to very short lifetimes. These searches would not be sensitive to long-lived heavy particles, which do not decay in the detectors. For example, heavy neutral singlet leptons with masses below 2 GeV will live long enough to escape the LEP and the SLAC Linear Collider detectors before decaying [30] and through their mixing they would contribute insignificantly to the width of the Z resonance and therefore would be they are disguised within the $N_\nu = 3$ light-neutrino number measurements [31]. These measurements also give a mass limit $M_L \gtrsim M_Z/2$ GeV. The disguise is not watertight from a theoretical point of view but this is of no experimental importance.

The possibility of light, long-lived new leptons has recently been addressed in [32] while [30] gives some older limits in the light of kaon decays, the absence of

forward neutral decaying particles in neutrino beams from conventional sources or beam dumps and high statistics neutrino experiments. Furthermore, singlet neutrinos do not have full couplings to the Z boson and would not contribute to the decay width of the Z, thus escaping detection.

Several models predict such long-lived particles. One example is the Minimal SuperSymmetric Model [33]. Some models beyond the Standard Model would also predict the existence of particles with fractional electric charge. As an example, leptoquarks [34] could be long-lived. There are also some long-lived hadronic states with fractional charge predicted by some modified Quantum Chromo Dynamics models [35].

1.5.1 Mixing

The *mixing* between a heavy fermion and an ordinary fermion (by Flavour Changing Neutral Currents) is parametrized by a constant ζ. In order to be general, this would have to be a mixing matrix containing the mixing between all the new fermions and the old ones ζ_{Ff} where F represents all the new fermions and f all the old ones. However, the intergenerational mixing is generally supposed to be very weak (see section 2.2). We will assume only one effective mixing parameter ζ for every new lepton. The mixing between fermions will alter their couplings to the electroweak

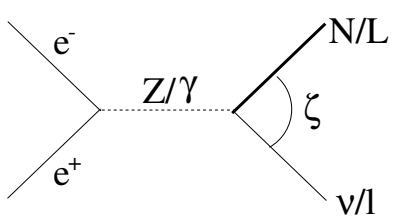

Figure 1-2: Mixing,ζ^2, between an ordinary and a heavy lepton.

gauge bosons ($Z, W^{\pm}, \gamma$). If this mixing is large, the high precision measurements[2] of the Z boson would be significantly altered, which is not the case. Thus, even the generational mixing must be rather small. The upper experimental limit on the mixing parameter is of the order of $\zeta^2 \lesssim 0.005$ [36, 37]. However, in some cases, the mixing could be higher [38]. If the left and the right-handed mixing angles are equal for leptons, their mixing can be even further constrained, to the order of $\zeta^2 \lesssim 0.0001$ [38]. This is due to the contributions from lepton loops to the anomalous magnetic moment $(g-2)_{e\mu}$, which would be too large unless the lepton mass is very large.

The decay length of the heavy neutrino is inversely proportional to the square of the mixing. If the mixing parameter is smaller than $\mathcal{O}(10^{-12})$ [15], the heavy neutrino is too long-lived to be discovered in the detector.

1.6 The Detector

1.6.1 The LEP Accelerator

The accelerator and storage ring had a circumference of about 27 km. Four experiments, called ALEPH, DELPHI, L3 and OPAL were placed equidistant along the ring[39]. The peak luminosity of the machine reached about 10^{32} cm^{-2}s^{-1}.

1.6.2 The OPAL Detector

This is a summary of the OPAL detector (see figure 1-3), the details can be found in [40].

[2]Measurements of total, partial and invisible decay widths as well as forward-backward and polarization asymmetries.

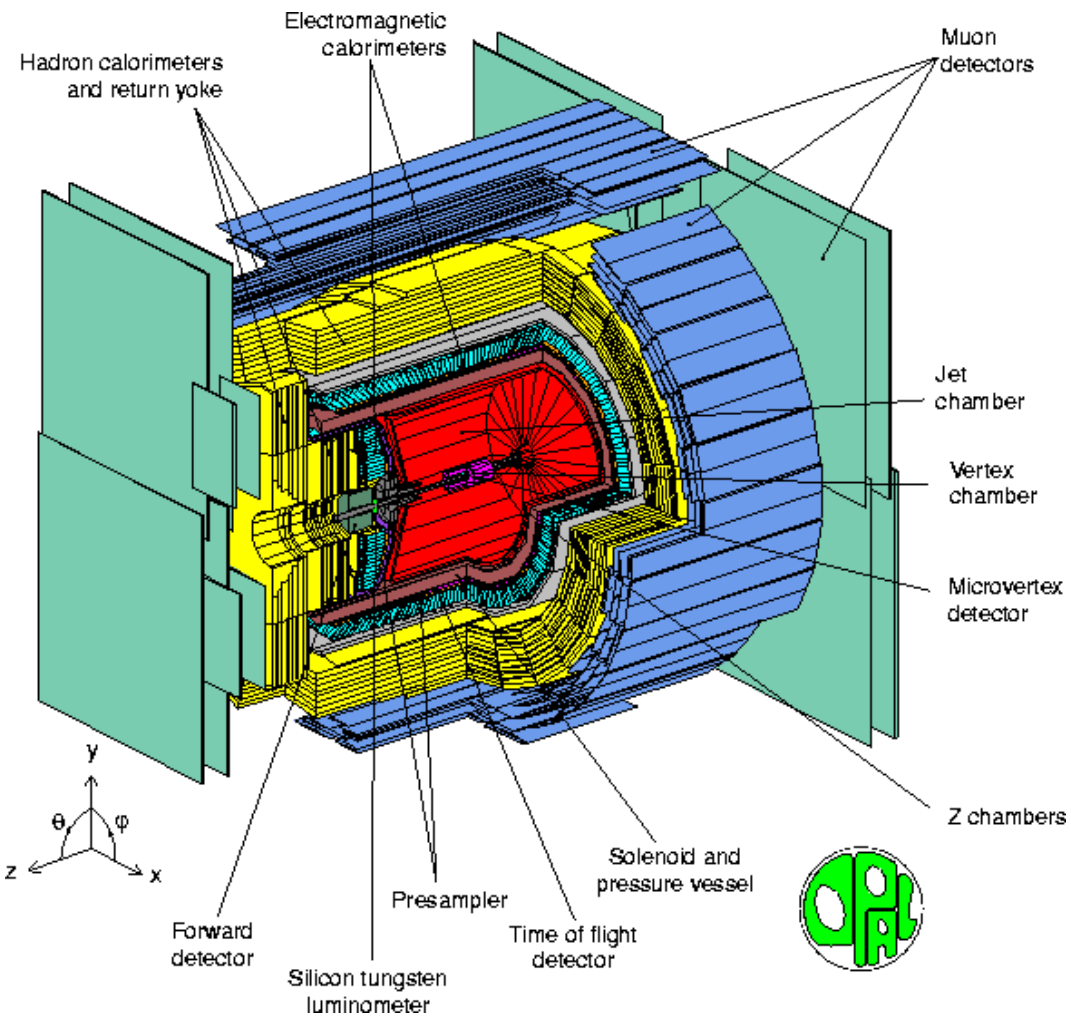

Figure 1-3: The OPAL detector

A trigger determines when a collision has occurred and causes the event to be recorded. It is set off when (i) an "essential" detector (such as the electromagnetic or hadronic calorimeters) detects a signal above a predetermined threshold or (ii) when a signal is observed in the same $\eta - \phi$ region (out of 6 η and 24 ϕ divisions) in a number of subdetectors.

The OPAL right-handed coordinate system is defined such that the z axis is in the direction of the electron beam, the x axis is horizontal and points towards the centre of the LEP ring, and θ and ϕ are the polar and azimuthal angles, respectively.

The OPAL detector consists of seven different parts:

- Central Detector
- Electromagnetic Calorimeter
- Hadron Calorimeter
- Muon Detector
- Forward Detector
- Silicon Tungsten Detector

a. Central Detector

The central detector consists of a system of tracking chambers, providing charged particle reconstruction over 96% of the full solid angle inside a 0.435 T uniform magnetic field. It consists of a two-layer silicon microstrip vertex detector, a high-precision drift chamber, a large-volume jet chamber and a set of Z-chambers measuring the track coordinates along the beam direction.

Closest to the interaction point is the microvertex detector to pin-point the earliest vertices. It is placed about 7 cm from the center of the beam pipe.

Then comes the vertex detector which is a jet-drift chamber providing track reconstruction with high precision. It has a radius of about 20 cm.

The jet chamber and the Z-chamber also do track reconstruction with the only difference that the Z-chamber only measures the z-coordinate of the tracks.

b. Electromagnetic Calorimeter

The electromagnetic calorimeter covers almost 99 % of the solid angle and can be used to identify electrons and photons.

The first part of this calorimeter is the time of flight chamber which permits low energy (0.6-2.5 GeV) charged particle identification.

Then comes presampling devices assuring the measurement of premature electromagnetic showers. After that the barrel lead glass calorimeter produces Cerenkov light used to identify the higher energy particles.

Finally there is an endcap presampler and calorimeter.

c. Hadron Calorimeter

The hadron calorimeter detects and measures the energy of jets, showers of particles concentrated in a specific direction. The jets are often the remnants of a quark.

d. Muon Detector

There are four muon detectors placed at the outer perimeter of the detector. A muon leaves an electromagnetic trace from the inner of the detector all the way out to the muon chamber. The muon is the only particle to do this since the other particles disintegrate before the muon chamber.

e. Silicon Tungsten Detector

The Silicon Tungsten Detector is an electromagnetic calorimeter used to measure the luminosity.

f. Forward Detector

Electromagnetic calorimeters close to the beam axis complete the geometrical acceptance down to 24 mrad on both sides of the interaction point.

Chapter 2

Phenomenology

2.1 Introduction

Basically there are two mutually supporting approaches relating physical principles, theory, and experiment. In the first approach, we start with some physical principles and from those we can deduce a theory. In our case we are concerned about the origin of the heavy leptons and the constitution of excited leptons. This part of the theory is briefly treated in chapter 1. In the second approach we investigate how our theoretical predictions would manifest themselves in experiments and we study the experimental parameters of the predictions. The latter approach will be presented in this chapter. Most of the properties are common to *exotic* (heavy or excited) leptons and quarks, even though the present thesis is concentrated on exotic leptons.

When the results are general, this will be made explicit by the use of the word fermion instead of lepton.

2.2 General

In LEP there are basically two ways of producing an exotic lepton. The first way is by single production, in which two electrons interact via a vector boson, which in turn decays into an exotic lepton and an ordinary lepton (see figure 2-1). The second one

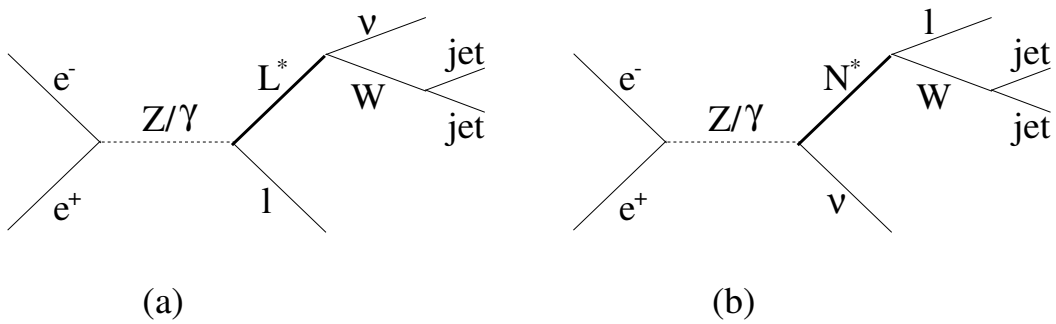

Figure 2-1: s-channel single production processes for heavy/excited fermions. (a) Charged exotic (heavy or excited) lepton, L^*. (b) Neutral exotic lepton, N^*.

is double production, in which the vector boson decays into a pair of exotic leptons (see figure 2-2).

If the mass difference between the exotic fermion and the ordinary fermion to which it decays, is less than the mass of the intermediary vector boson, the latter is virtual, leading to a three body final state. Otherwise, the boson is real, giving a two-body phase space for the decay.

The general formulae for heavy fermions are described in [41]. These formulae account for single production of these heavy fermions as well as for double production of them including all possible decay channels for the different types of fermions (as described in 1.4). The exotic fermions have electromagnetic and weak couplings, except for the singlet neutrinos which only couple through the mixing. The Lagrangian of the interactions of the new fermions is:

$$L = \sum_{V=\gamma,Z,W^{\pm},...?} g_V J_V^{\mu} V_{\mu} \tag{2.1}$$

where implicit summation over μ is assumed, V_μ is the four vector of the vector boson field V, J_V^μ is the fermion current coupling to V and complex conjugation of the charged current is understood. V allows for Standard Model as well as new vector bosons.

g_V are the coupling constants:

$$g_\gamma = e, \quad g_Z = \frac{e}{\sin\theta_W \cos\theta_W}, \quad g_W = \frac{\sqrt{2}e}{\sin\theta_W} \tag{2.2}$$

for the Standard Model vector bosons. In this thesis, it will be supposed that any new gauge boson will be heavy enough not to affect the result. Furthermore, it is also supposed that the mixing between the new vector bosons and the Z is too weak to interfere with the current research.

A coupling ζ allows the *mixing* between the exotic fermions and the ordinary fermions. In this thesis, the mixing is supposed not to be intergenerational. In other words, a heavy fermion of electron-type would not mix with the regular muon, tauon, their neutrinos or the quarks. This is motivated by the fact that large intergenerational mixing would introduce flavour changing neutral currents at tree level. However, these currents are severely limited by experimental data [6], thus putting a tight constraint on intergenerational mixing.

2.2.1 Comments About Cross Section Generation

In order to generate the cross sections in the sections below, a number of (rather general) conditions have been taken into account. Spin-correlations have been included as well as initial state radiation. Final state radiation has not been used, due to limitations in the EXOTIC [42] software. The effect has, however, been shown to be negligible [43]. The fermions that interest us are leptonic, and they are all supposed to belong to the first generation because their cross sections are much higher than in the second and third generationi, [41].

For heavy leptons, the mixing angle has been taken as $\zeta^2 = 0.005$, and for excited leptons the gauge coupling parameters $f = f' = 1$ (see section 2.4.3).

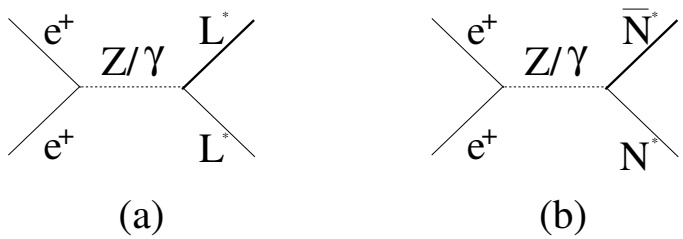

Figure 2-2: s-channel double production processes for heavy/excited fermions. (a) Charged exotic leptons, L^*. (b) Neutral exotic leptons, N^*.

2.3 Double Production of Exotic Leptons

Pair production of heavy leptons is mainly achieved through the s-channel (see figure 2-2) via a virtual photon or Z^0. There is also a contribution from the t-channel but it is quadratically suppressed [41] by the mixing angle and is very small. Masses up to $\sqrt{\hat{s}}/2$ can be probed in double production.

The principal production channels are:

$$e^+e^- \to E^+E^- \to e^+e^-ZZ \to e^+e^- + 4\,\text{jets}$$

$$e^+e^- \to N\bar{N} \to e^+e^-WW \to e^+e^- + 4\,\text{jets}.$$

W/Z leptonic decay has a comparatively low branching ratio, and the neutrino identification can be problematic.

The unpolarized differential cross section for pair production of heavy leptons is:

$$\frac{d\sigma}{d\cos\theta} = \frac{3}{8}\sigma_0 N_c \beta_F \left[(1+\beta_F^2\cos^2\theta)Q_1 + (1-\beta_F^2)Q_2 + 2\beta_F\cos\theta Q_3\right], \tag{2.3}$$

where $\sigma_0 = 4\pi\alpha^2/3s$, $s = (\ell+\bar{\ell})^2$, ℓ is the four vector of the ordinary lepton, $\beta_F = \sqrt{(}1-4m^2/s)$ (velocity of the final state fermion), m is the mass of the fermion, and N_c is the number of colours, i. e. three for quarks and one for leptons. The

generalized charges Q_i are rather comlicated and can be found in equation (3.4) in [41].

The cross section is plotted in figure 2-3.

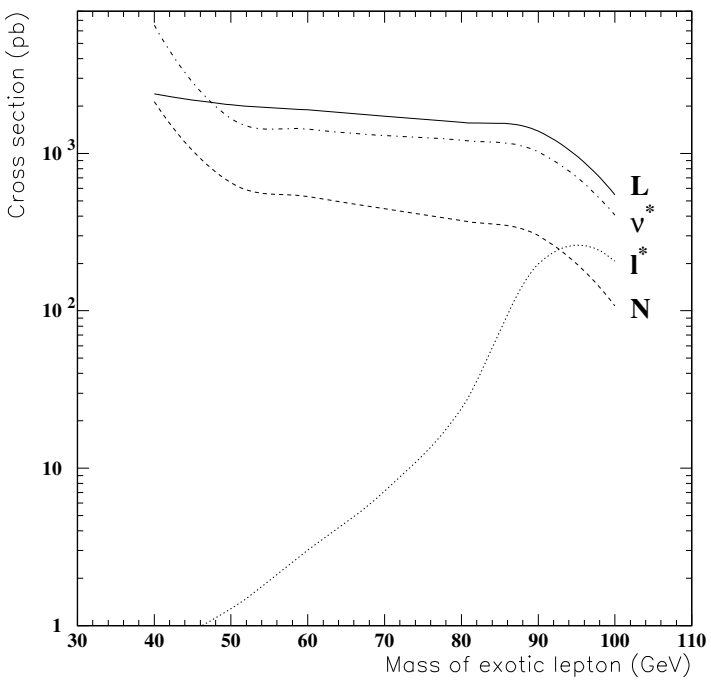

Figure 2-3: Cross sections for double production of different types of exotic leptons at $E_{CMS} = 207$ GeV. All the types of heavy charged leptons, L, have the same cross section σ_L and all the types of heavy neutral leptons, N, have the same cross section σ_N. The different types of heavy leptons are discribed in section 1.4. The heavy lepton case assumes a mixing angle $\zeta^2 = 0.005$. The excited lepton case assumes a mass scale $\Lambda^2 = 1$ TeV and $f = f' = 1$ (see section 2.4.3). problems.

In this thesis there is only a general discussion on double production of exotic leptons, as the data has already been analysed in detail in [19].

2.4 Single Production of Exotic Leptons

For exotic quarks and second and third generation leptons, single production proceeds only through the s-channel [44]. This means that a photon or a Z^0 splits into an exotic fermion and an ordinary one. However, for the electron type, additional t-channel production is allowed (see figure 2-4). This means W exchange for neutral leptons and Z exchange for charged leptons. The t-channel is obviously not available for muon- and tau-type heavy leptons because LEP is an e^+e^- collider. The t-channel increases the cross section by several orders of magnitude making a search for electron-type heavy leptons favourable.

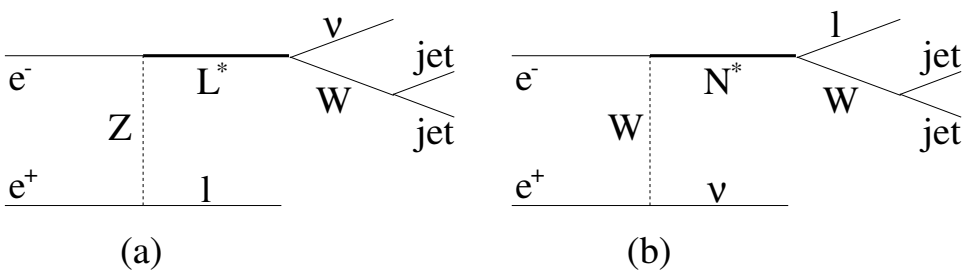

Figure 2-4: t-channel single production processes for heavy/excited fermions. (a) Charged exotic lepton, L^*. (b) Neutral exotic lepton, N^*.

For single production of heavy fermions to be possible, there has to be a mixing between the ordinary and the exotic fermions. Otherwise, flavour conservation would make the production impossible.

The heavy fermions decay into their light counterparts and a vector boson, again through mixing. Thus, the final state is rather complicated, containing four different particles. However, the final state particles are not distributed randomly. This is a fact that can be used to distinguish them from the background noise. Their distribution pattern and properties of the decay particles can also help us to identify the type of the heavy lepton (see section 1.4), which is crucial to the understanding of the origin of heavy leptons. In particular, the angular distributions are useful for this purpose [44] as the different types of heavy leptons have the same type of interaction, differing

only in their angular distributions.

The calculated cross sections for different signals are given in figures 2-5 and 2-6, presenting the cross section as a function of mass and energy, respectively. The cross section for masses close to the Z^0 mass, is not well treated by the inital state radiation method (PHOTOS [45] used by EXOTIC [42]) for single production of exotic leptons.

A rough estimate for the number of expected events for a total integrated luminosity of 660 pb^{-1} would be:

ℓ^* : 660 L : 2

ν^* : 15 N : 100

supposing the mass of the exotic fermion to be 140 GeV and the center of mass energy to be 200 GeV. However, at such a low mass, the cross section will be roughly the same for the different center of mass energies (see table 2-I).

This cross section as a function of energy is plotted in figure 2-6.

2.4.1 Branching Ratio $\Gamma_{CC/NC}$

The branching ratio for heavy fermion decay through the charged current (decay through $W^{\pm}$) versus the neutral current (decay through Z^0) is independent of the center of mass energy, as well as of type and charge of the exotic lepton. This result has been obtained with EXOTIC [42] which is based on the formulae in [44].

The expressions for the partial decay widths for on-shell vector bosons are:

$$\Gamma(F_{L,R} \to Zf) = \frac{\alpha}{32\sin^2\theta_W\cos^2\theta_W}(\zeta^{fF}_{L,R})^2\frac{m_F^3}{M_Z^2}(1-v_Z)^2(1+2v_Z) \quad (2.4)$$

$$\Gamma(F_{L,R} \to Wf) = \frac{\alpha}{16\sin^2\theta_W\cos^2\theta_W}(\zeta^{fF}_{L,R})^2\frac{m_F^3}{M_W^2}(1-v_W)^2(1+2v_W) \quad (2.5)$$

where $v_{W,Z} = (M_{W,Z}/m_F)^2$ and $\Gamma_{tot} = \Gamma_{CC} + \Gamma_{NC}$. This means that for low fermion masses m_F, the charged current channel will be strongly dominating, and even when

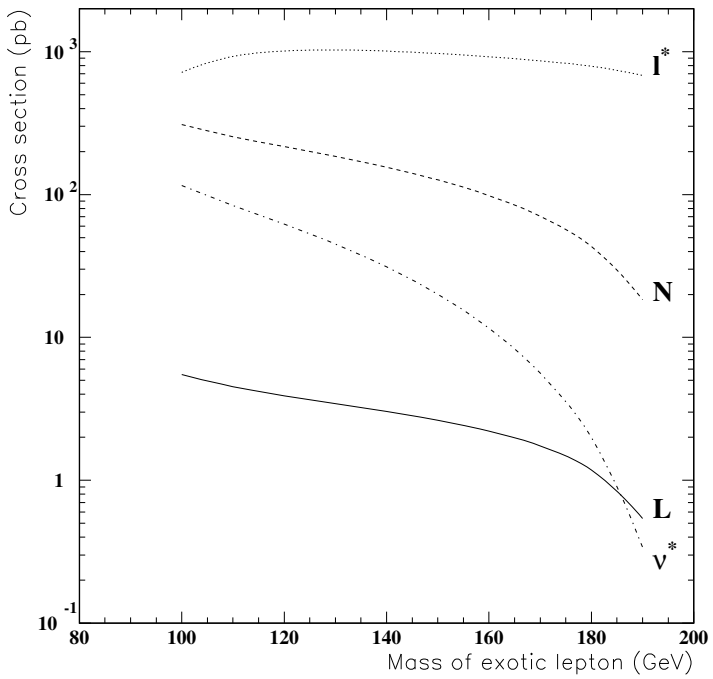

Figure 2-5: Cross sections for single production of different types of exotic leptons at $E_{CMS} = 200$ GeV. All the different types of heavy leptons (as described in section 1.4) have the same cross section. The heavy lepton case supposes a mixing angle $\zeta^2 = 0.005$.

$m_F >> m_{W,Z}$ the charged current channel will have twice as high a cross section.

2.4.2 Heavy Leptons

The polarized cross section of a heavy lepton is given by

$$\frac{d\sigma^{\text{unpol}}}{d\cos\theta} = \frac{3}{8}\sigma_0 N_c \beta_F \left[(1+\beta_F^2\cos^2\theta)Q_1 + (1-\beta_F^2)Q_2 + 2\beta_F\cos\theta Q_3\right] \tag{2.6}$$

where $\sigma_0 = 4\pi\alpha^2/3s$, $s = (\ell + \bar{\ell})^2$ and $\beta_F = \sqrt{1-4m^2/s}$ and N_c is the number of colours, i. e. three for quarks and one for leptons. The values of the cross section are presented in table 2-I.

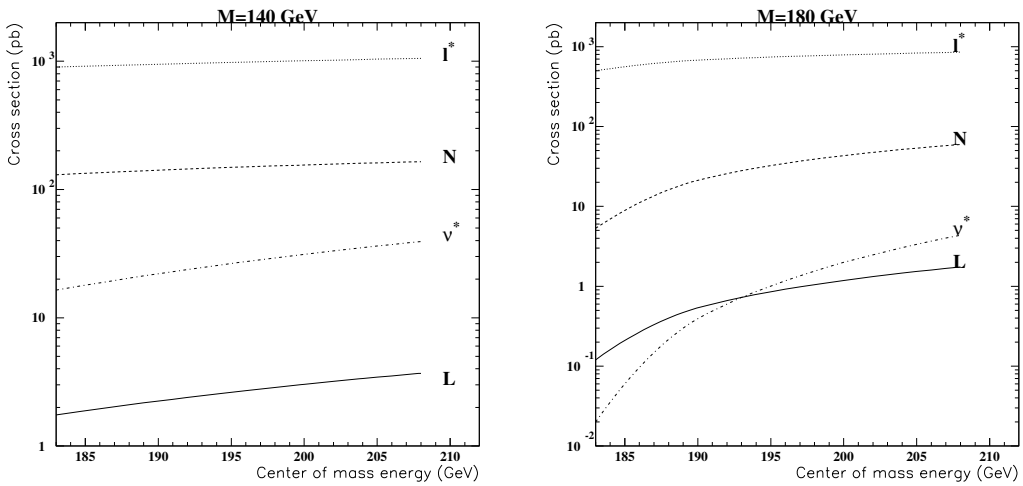

Figure 2-6: Cross sections for single production of different types of exotic leptons as a function of energy. All the types of heavy leptons have the same cross section. The heavy lepton case supposes a mixing angle $\zeta^2 = 0.005$.

Mass:	100	110	120	130	140	150	160	170
$\sigma_{\sqrt{\hat{s}}=183}$	305.42	245.44	202.14	165.09	130.24	96.34	63.42	32.15
$\sigma_{\sqrt{\hat{s}}=189}$	306.62	248.80	207.63	172.70	139.96	108.09	76.90	46.66
$\sigma_{\sqrt{\hat{s}}=192}$	307.25	250.41	210.17	176.21	144.42	113.48	83.14	53.50
$\sigma_{\sqrt{\hat{s}}=196}$	308.12	252.46	213.37	180.60	150.01	120.24	90.98	62.20
$\sigma_{\sqrt{\hat{s}}=200}$	309.05	254.45	216.41	184.73	155.24	126.56	98.35	70.41
$\sigma_{\sqrt{\hat{s}}=202}$	309.51	255.41	217.88	186.70	157.74	129.58	101.86	74.36
$\sigma_{\sqrt{\hat{s}}=204}$	310.01	256.37	219.31	188.63	160.17	132.51	105.27	78.19
$\sigma_{\sqrt{\hat{s}}=205}$	310.24	256.84	220.02	189.56	161.35	133.93	106.94	80.08
$\sigma_{\sqrt{\hat{s}}=206}$	310.49	257.30	220.72	190.49	162.52	135.35	108.58	81.93
$\sigma_{\sqrt{\hat{s}}=207}$	310.74	257.79	221.40	191.42	163.66	136.73	110.20	83.76
$\sigma_{\sqrt{\hat{s}}=208}$	311.00	258.24	222.09	192.32	164.80	138.10	111.80	85.56

Table 2-I: Cross sections, σ_j (pb) for single heavy neutrino production for different masses, M_N (GeV) and center of mass energies, $\sqrt{\hat{s}}$ (GeV).

a. Decay

The possible decay channels for a heavy lepton are:

$$\mathrm{N} \to \ell^{\pm}\mathrm{W}^{\mp} \quad , \quad \mathrm{N} \to \mathrm{L}^{\pm}\mathrm{W}^{\mp} \quad , \quad \mathrm{N} \to \nu_{\ell}\mathrm{Z},$$

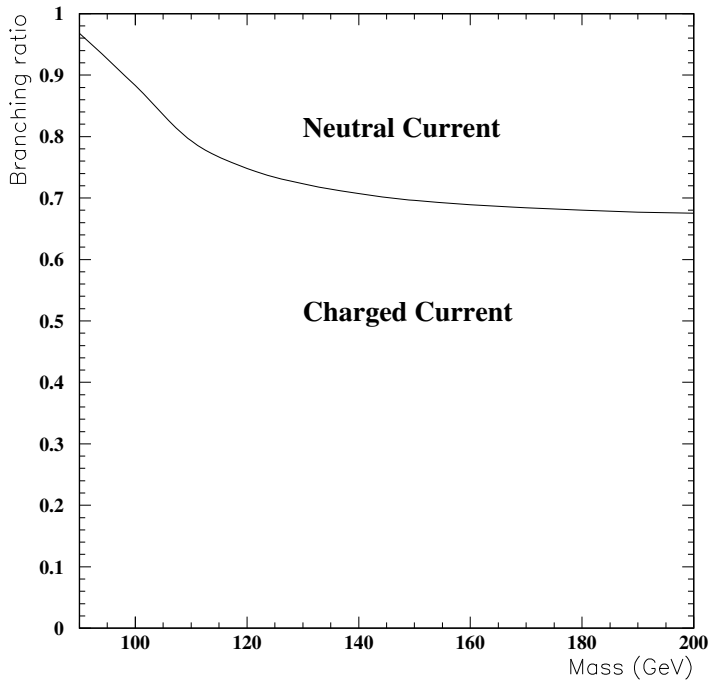

Figure 2-7: Branching ratio $L \to W/Z + \ell$ for single production of heavy leptons as a function of energy. All the types of heavy leptons, charged as well as neutral, have the same branching ratio.

$$\mathrm{L}^{\pm} \to \nu_{\ell}\mathrm{W}^{\pm} \quad , \quad \mathrm{L}^{\pm} \to \mathrm{NW}^{\pm} \quad , \quad \mathrm{L}^{\pm} \to \ell^{\pm}\mathrm{Z}.$$

The decay of a heavy fermion into another (lighter) heavy fermion is possible, though not favourable, because of their smaller mass difference compared to that between a heavy and an ordinary lepton. However, if the mixing angle ζ^2 is very small, decay into another heavy lepton could still be a possibility. From the fact that the charged leptons in general are much heavier than their neutral counterparts, it is plausible that the same would be the case for heavy leptons. In this case, the channel $N \to L^{\pm}W^{\mp}$ would be kinematically closed.

2.4.3 Excited Leptons

Excited leptons are supposed to have the same electroweak $SU(2)\times U(1)$ couplings (g and g') as ordinary leptons. However, unlike ordinary leptons, they are supposed to be grouped into both left-handed and right-handed iso-doublets with vector couplings to the gauge bosons (Vf^*f^*). The Vf^*f^* coupling is of magnetic type. If the excited leptons were not iso-doublets, the light leptons would radiatively acquire a large anomalous magnetic moment, due to the $\ell^*\ell V$ ($V = Z, W, \gamma$) interaction [46].

The effective Lagrangian of excited leptons is [46]:

$$\mathcal{L}_{\ell\ell^*} = \frac{1}{2\Lambda}\bar{\ell}^*\sigma^{\mu\nu}\left[gf\frac{\boldsymbol{\tau}}{2}\mathbf{W}_{\mu\nu} + g'f'\frac{Y}{2}B_{\mu\nu}\right]\ell_{\mathrm{L}} + \text{hermitian conjugate}, \tag{2.7}$$

which describes the generalized magnetic de-excitation of the excited states through the decay of the excited lepton. The matrix $\sigma^{\mu\nu}$ is the covariant bilinear tensor, $\boldsymbol{\tau}$ are the Pauli matrices, $\mathbf{W}_{\mu\nu}$ and $B_{\mu\nu}$ represent the fully gauge-invariant field tensors, and Y is the weak hypercharge. The parameter Λ has units of energy and can be regarded as the compositeness scale, while f and f' are the weights associated with the different gauge groups. The relative values of f and f' also affect the size of the single-production cross-sections and their detection efficiencies. Either the photonic decay, the CC decay, or the NC decay will have the largest branching fraction, depending on their respective couplings [46]:

$$f_\gamma = e_f f' + I_{3L}(f - f') \quad , \quad f_W = \frac{f}{\sqrt{2}s_w} \quad , \quad f_Z = \frac{4I_{3L}(c_w^2 f + s_w^2 f') - 4e_f s_w^2 f'}{4s_w c_w}$$

where e_f is the excited fermion charge, I_{3L} is the weak isospin, and $s_w(c_w)$ are the sine (cosine) of the Weinberg angle θ_w.

The integrated cross section for excited leptons is plotted as a function of mass and energy in figures 2-5 and 2-6 respectively.

The possible decay modes for an excited lepton are:

$$\nu_\ell^* \to \nu_\ell\gamma \quad , \quad \nu_\ell^* \to \ell^\pm \mathrm{W}^\mp \quad , \quad \nu_\ell^* \to \nu_\ell \mathrm{Z},$$

$$\ell^{*\pm} \to \ell^{\pm}\gamma \qquad , \qquad \ell^{*\pm} \to \nu_{\ell}\mathrm{W}^{\pm} \qquad , \qquad \ell^{*\pm} \to \ell^{\pm}\mathrm{Z}.$$

Chapter 3

Simulation and Selection

3.1 Introduction

This chapter describes the Monte Carlo generated signals of exotic leptons and their background. It also includes cut-optimization, which is applied on the Monte Carlo samples in order not to be biased by the data. The Monte Carlo samples have been generated for several different energies and normalized with respect to the corresponding integrated luminosity at LEP (see table 3-I). Furthermore, they have been grouped into three regions, 183-189 GeV, 192-200 GeV and 202-209 GeV. There are two reasons for this grouping. The first reason is that the cross sections of the sought signals is so small that statistically, they would not show at one single energy. The second is that the grouping simpifies the calculations. The total integrated luminosity is 663 pb^{-1} after detector cuts. Detector cuts means basically that all detectors are required to have registered a clean signal.

E_{CMS} [GeV]	183	189	192	196	200	202	204	205	206	207	208
$\int \mathcal{L}dt$ [pb^{-1}]	57.3	187	28.7	71.1	74.3	38.1	6.5	69.6	16.6	106	7.7
$\Sigma \int \mathcal{L}dt$	244.5		174.0			244.9					

Table 3-I: Integrated luminosities at LEP for different center of mass energies. The total integrated luminosity, $\Sigma \int \mathcal{L}dt = 663.5$ pb^{-1}. The energies in the center of mass system are approximate within 1-2 GeV.

After having been generated, all Monte Carlo events (both signals and backgrounds as described later) are processed through the GOPAL [47] system, which is

a detector simulator based on GEANT 3. GEANT provides tools to allow the user to define the geometrical parameters of his detector, using standard shapes. GEANT also deals with tracking of particles through this detector, including the necessary physics processes (scattering, decays, interactions). All Monte Carlo results (and later on also the data) are then processed through the same system of pre-selection.[1] and then through selection of events with desired characteristics. The detector itself is described briefly in section 1.6.

3.2 Signal Generation

The simulation of the signal have been done with EXOTIC [42], a Monte Carlo generator for single and pair production of heavy and excited fermions in e^+e^- colliders. All spin correlations in the production and in the decay processes are included, as well as the transition betweeen a virtual and a real intermediate vector boson at $M_N \sim M_Z, M_W$. The hadronization of quarks is done with the JETSET [48] package. The formulae for the generation of exotic fermions are based on [41, 50].

EXOTIC was chosen because it is the most versatile generator. For heavy leptons, TIPTOP [51] is another possible generator, but it is more limited. It only generates pair-produced sequential leptons within the framework of the Standard Model. PYTHIA [49] could also have been used, but it is restrained to generate fourth generation sequential fermions and it does not include spin-correlations.

For the generation of excited fermions, existing Monte Carlo generators do not take into account the polarization of the ℓ^* in their decay process which is important for the angular distribution of ℓ^*. Besides, decays via Z^0 and W have not been considered. For further discussion on the limits of alternative generators, see the EXOTIC write-up [42].

[1] The pre-selection scheme is named the Tokyo Multihadronic Event Selection (TKMH) [53] and basically means that only good multihadronic events are kept.

Within the OPAL collaboration, several topics have already been covered, like heavy lepton double production [19] and excited leptons with photon decay [52]. For further discussions see chapter 1.

The assumptions made for the signal generation are summarized and motivated in the following sections.

3.2.1 General

- Leptons, not fermions
  The fact that the accelerator collides e^+e^- favours the production of leptons. Exotic quarks might also be produced, but we know that a fourth quark would have to be heavier than the top quark and therefore it would not be observable (see however [54]).

- Single production for $M > 100$ GeV
  This thesis is primarily focused on single production, because the final state $(jj\ell\nu)$ is clean and easy to identify. Furthermore, double production of heavy leptons is already covered by [19] up to heavy lepton mass 103 GeV.

- Charged Current Channel
  The charged current channel is selected in preference to the neutral current channel, due to its higher branching ratio. Even for high masses, the branching ratio into a W is roughly double that into a Z^0. For further details, see figure 2-7.

- $W \to jj$
  The branching ratio of $W \to jj$ is about 70 %, while the branching ratio of $W \to \ell\nu$ is about 20 % (not counting the τ neutrino, which is not easily identified). Further, the final state signature $\ell\nu jj$ is rather easy to identify and to reconstruct. Using the $W \to \ell\nu$ channel would imply a combinatory problem between the two leptons, as well as it would lead to severe difficulties

in distinguishing the neutrinos.

- Minimum cross section 15 fb

  If the number of signal events is required to be at least ten, then the smallest allowed cross section is $\sigma \gtrsim 15$ fb for the total integrated luminosity of 663.5 pb^{-1}. If the number of signal events is significantly lower than ten they will most likely disappear during the cuts.

- No final state radiation in EXOTIC

  There is a bug in the OPAL version of the code of EXOTIC making it impossible to use final state radiation. The effect, however, has been found to be small, [43].

  For masses around 90 GeV, even the initial state radiation encounters some difficulties, thus producing unphysical results. This is due to the transition between a three body problem with a virtual vector boson, and a two body problem with a real vector boson at the Z^0 peak ($M \sim 90$ GeV). Further discussion can be found under the section ISRGEN in [42].

- The use of spin correlations.

  This means that the angular distributions should be correctly generated.

- No new vector bosons light enough to affect the results.

3.2.2 Heavy Leptons

- Heavy electron generation, neither heavy μ, nor heavy τ.

  As we have mentioned in chapter 1 intergenerational mixing is assumed not to exist. Futhermore, only the first generation is studied, due to the non-existence of the t-channel in the other generations. The t-channel gives a much higher contribution to the cross section than the s-channel. For example, in the second generation, the number of observed events can be predicted to peak at about three, which would be hidden by the LEP background (see chapter 2).

- $\zeta_L^2 = \zeta_R^2 = 0.005$
  The current upper limit on the *mixing* of heavy leptons and ordinary leptons (see section 1.5.1).
- Assuming $M_L > M_N$ so that the channel $N \to L^{\pm}\ell^{\mp}$ is kinematically closed.
- Left-handedness
  There is no major difference between right-handed and left-handed leptons, except in the θ distribution for heavy neutrinos. The left-handed state has been chosen in order to limit the calculations.

3.2.3 Excited Leptons

- Only generation of e^*, not μ^* or τ^*.
  The electrons are the easiest to detect and identify.
- The gauge coupling parameters $f = f' = 1$.
  As an extension to the current study, the case where $f = -f' = 1$ could be studied.
- The compositeness scale is, rather aritrarily, set to $\Lambda = 1$ TeV.
  The cross section is inversely proportional to the square of the mass scale.

3.3 Backgrounds

The backgrounds that are likely to cloud the signature of the signal (electron, neutrino and two jets) are (ordered approximately by importance as can be seen in tables 3-VIII and 3-IX):

1. llqq
   This is an irreducible background as it has exactly the same signature as the

signal. The main production process is $WW, ZZ \rightarrow$ llqq. For technical reasons the eeqq background has been generated and treated separately.

2. qq(γ)
   The cross section of this process is very high but on the other hand, the final state is quite different from the final state of the signal. in order to confuse the two of them, the lepton must come e. g. from one of the jets (b-jet or c-jet) and the missing energy could come in the form of radiation or a particle disappearing along the beampipe. The production process is $Z/\gamma^* \rightarrow$ qq.

3. qqqq
   Two showers are recognized as jets, while the other two give rise to individual particles. Some of these include leptons and neutrinos, which is the signature of the signal. The principal sources of this background are $WW, ZZ \rightarrow$ qqqq.

4. $\gamma^*\gamma$qq
   If one of the electrons from $e^+e^- \rightarrow e^+e^-\gamma^*\gamma \rightarrow e^+e^-qq$ is undetected, then this final state correspond to that of the signal. $\gamma\gamma$qq has not been considered, due to the fact that the virtuality of the photons must be rather high.

5. ee$\tau\tau$
   The two τ decay quickly to produce the jets and missing energy. $\gamma\gamma\tau\tau$ has not been included because of its rather far-fetched signature.

The explanations above show how the backgrounds can be confounded with the signals. Note, however, that they are only examples and that other confusions also are possible.

The backgrounds have been generated by the OPAL collaboration with KK2f [55], Pythia [49] PHOJET [56] and grc4f [57] (cf. table 3-II).

Alternatively, a number of other generators could have been used, for instance KORALW [58] for the llqq and qqqq backgrounds.

The $\gamma\gamma$qq (where γ is a real photon) background has not been considered due to the fact that the virtuality of the photons must be rather high to be a real background to our process. Even when one of the photons can be considered to be virtual, the background is hardly noticeable (see table 3-IV).

The $\ell\ell\ell\ell$ background has not be treated either because of its relatively low cross section ($\sim$ 3 pb) in combination with the remoteness of the final state particles compared to the signal.

Bg	**Generator**	**Simulated events/energy**
qq(γ)	KK2f/PY6.125	200k ($\sim$2 fb^{-1})
llqq	grc4f 2.1	5 fb^{-1}
eeqq	grc4f 2.1	5 fb^{-1}
qqqq	grc4f 2.1	5 fb^{-1}
ee$\tau\tau$	grc4f 2.1	5 fb^{-1}
$\gamma^*\gamma qq$	HERWIG	150k-350k ($\sim$.5-1 fb^{-1})

Table 3-II: Background processes. The $\gamma^*\gamma qq$ background has 150k events for E=183, 189, 196 and 200 GeV; 350k events for E=192, 202, 204, 205, 207, 208 GeV and 330k events for E=206 GeV.

E_{CMS}	183	189	192	196	200	202	204	205	206	207	208
$\sigma_{qq\gamma}$ [pb]	109	99.4	94.8	90.1	85.6	83.4	82.1	81.3	79.5	79.4	78.4
σ_{llqq} [pb]	8.11	8.68	8.95	9.14	9.28	9.32	9.37	9.39	9.40	9.42	9.43
σ_{eeqq} [pb]	26.7	25.5	41.4	40.5	39.5	39.0	38.7	38.3	38.2	38.1	37.8
σ_{qqqq} [pb]	7.86	8.42	8.66	8.82	8.91	8.94	8.96	8.97	8.97	8.97	8.97
$\sigma_{ee\tau\tau}$ [pb]	1.88	1.83	1.82	1.80	1.78	1.75	1.75	1.74	1.74	1.73	1.73
$\sigma_{\gamma^*\gamma qq}$ [pb]	296	302	310	310	314	321	324	325	326	327	328

Table 3-III: Cross sections for background processes for different energies. Energy given in GeV. There are no simulations for $203, 209$ GeV, but their luminosities are so low that it does not matter.

For specific energies, where the luminosity is high and the number of generated events are low, the number of generated background events might be insufficient.

Notably, this is the case for the $\gamma^*\gamma qq$ background, where the 189 GeV energy is particularly flagrant. The number of generated events correspond to a luminosity of about 500 pb^{-1} while the data contains roughly 200 pb^{-1}. Unfortunately, at this moment, there are no more of these background events available. However, this background is very sensitive to the preliminary cuts (see section 3.4.2) and is quickly eliminated. This means that the lack of simulations is not really a problem.

The only other background where simulations might be insufficient is the qq(γ) final state. In the worst case (at $E = 189$ GeV), the number of generated events correspond to about 2 fb^{-1}, which is ten times the data luminosity. This should be rather sufficient.

3.4 Variables and Cuts

3.4.1 Description of Variables

The electron mentioned below refers to the most energetic electron detected, while the neutrino is deduced as the missing energy and momentum. The missing energy and momentum can either be a neutrino, which passes right through the detector, or particles that pass so close to the beam pipe that they escape detection. Often it is both, making the determination of the exact neutrino energy and momentum difficult. The W is reconstructed from the two jets. The jets are identified with the Durham jet-finding algorithm [59] forcing reconstruction of only two jets. The quality of this jet-finding is characterized by y_{12} but this variable has not proved to be of any use in the cuts.

- $|\cos\theta_{\text{vis}}|$

θ_{vis} is the angle between the missing[2] momentum and the z-axis. 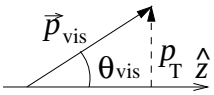

- $M_{\ell\nu}$

  is the reconstructed invariant mass of the neutrino and the lepton with the highest energies. This variable will have a peak around $M_W = 80$ GeV for all backgrounds containing W. This means that it is very useful to eliminate the llqq background.

- E_ν

  is the energy of the neutrino, which is reconstructed supposing that there are only two jets and one charged lepton except for the neutrino. This variable is very useful to eliminate the qq(γ) background.

- E_ℓ

  is the energy of the most energetic lepton, which should be the lepton shown in figure 2-1. Unfortunately this is not always the case (cf. 3.6). This variable is very useful to eliminate the qq(γ) background.

- M_N

  is the mass of the reconstructed neutral lepton (N), i. e. the invariant mass of the two jets and the most energetic lepton.

- M_L

  is the mass of the reconstructed charged lepton ($L^\pm$), i. e. the invariant mass of the two jets and the most energetic neutrino (missing $E, \vec{p}$).

- $\theta_{W\ell}$

  is the angle between electron and the W direction in the center of mass system of the reconstructed W. 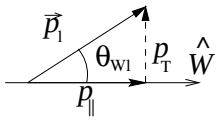

- $\theta_{Wl\nu}(\hat{z})$

  is the angle between the reconstruced W and the invariant $l\nu$ in the laboratory

[2] Conservation of momentum gives that $\vec{p}_{\text{missing}} = -\vec{p}_{\text{visible}}$ and thus $\theta_{\text{vis}} = \pi - \theta_{\text{mis}}$.

coordinate system. This variable could be used to discriminate the signal from the irreducible WW background. 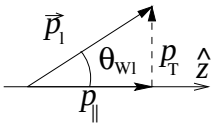

- $\theta_{N\ell}$
  is the angle between the reconstructed N and the ℓ in the coordinate system of the reconstructed N. This variable has not proved to be very useful to distinguish the signal from the background, but it might, for example, be used to distinguish the type of heavy lepton. 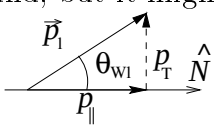

- Lepton type
  is useful to distinguish heavy leptons, which should basically only give electron-type recoil leptons.

Note that the angle variables make sense in the heavy neutral lepton case. This is also the only case that has been studied thoroughly.

3.4.2 Preliminary Cuts

First of all, a standard set of OPAL cuts is applied on the Monte Carlo samples, the Tokyo Multihadronic Event Selection [53]. These cuts are applied in order to have nice jets, which is advantageous in the present analysis.

As seen in section 3.3, the backgrounds that have only photons and/or quarks in their final state have a rather high cross section. However, due to the lack of leptons, these backgrounds can be severely reduced by requiring a high energy of the lepton and of the neutrino. All the signals of exotic neutrinos have rather high E_ℓ and E_ν because of their kinematics. However, the heavier the exotic lepton is, the more energy is available for the recoil lepton and the less for the neutrino. It would eventually be

possible to combine these two variables and cut only on the combination as the two energies are kinematically interrelated. For the moment, cutting each one individually still produces good results.

For all exotic neutrinos and their backgrounds, the following preiminary cuts have been applied:

$$E_\nu > 10\,\mathrm{GeV}, \qquad E_\ell > 5\,\mathrm{GeV}.$$

These cuts reduce the signals with a factor of about 1.3-1.5 (depending on the mass of the exotic lepton) while the quark backgrounds mentioned above are reduced more than sevenfold. The other backgrounds are moderately reduced as can be seen in table 3-IV.

Process	Reduction	# of events after prel. cuts
qq(γ)	7.57	9787
llqq	1.88	23002
eeqq	2.78	3571
qqqq	7.51	5868
ee$\tau\tau$	1.56	37
$\gamma^*\gamma qq$	7.4	64

Table 3-IV: The effect of the preliminary cuts. The reduction is defined as the number of events before divided by the number of events after the preliminary cuts.

3.5 Complete Analysis of Heavy Neutrinos

Heavy neutrinos have been extensively studied for $M_N = 100$, 110, 120, 130, 140, 150, 160, 170 GeV. Higher masses have not been studied due to the difficulties present already at 170 GeV (see table 4-II). It is noteworthy that the masses are high enough

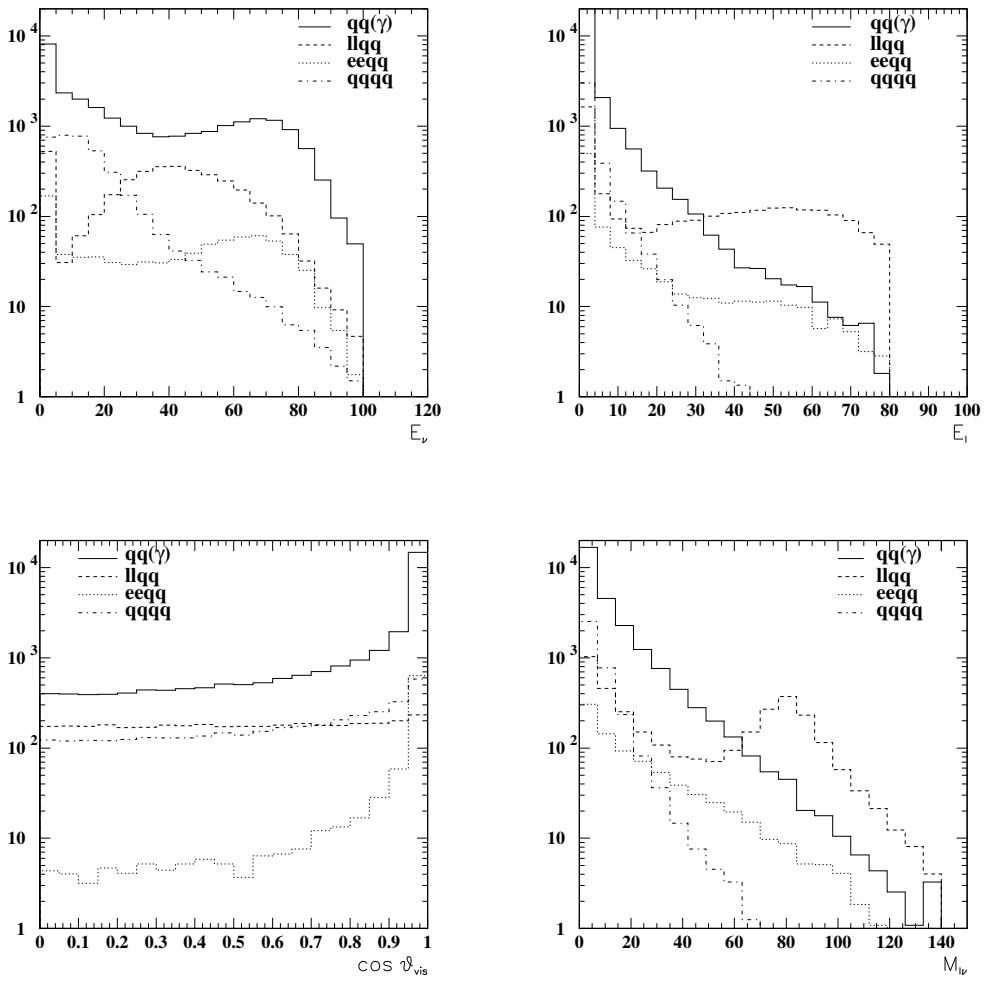

Figure 3-1: Comparison of the principal variables for different backgrounds. The integrated luminosity $\int \mathcal{L}dt = 79.3$ pb^{-1} and the center of mass energy $E_{CMS} = 200$ GeV.

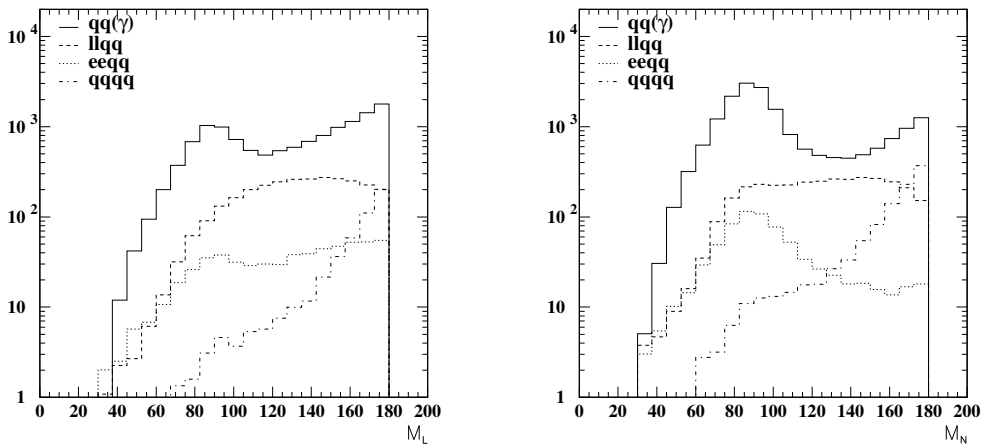

Figure 3-2: Comparison of reconstructed masses M_L and M_N for different backgrounds

to avoid the problems with initial state radiation, as has been discussed in section 3.2. Each mass and energy region has been individually treated and optimized.

The analysis has been divided into three energy regions in order to optimize the different cuts more effectively. The first region is 180-190 GeV, containing 244.5 pb^{-1}, the second region is 191-200 GeV, containing 174.04 pb^{-1}, and the last region is 201-209 GeV. containing 244.92 pb^{-1}.

3.5.1 Cuts

There are many different methods to optimize the cuts. It matters in what order the cuts are applied. It also matters whether all optimizing cuts are applied at the same time, or if they are applied one by one, with an inspection of the results before moving on to the next cut. Different methods give different results although the conclusions have proved to be basically the same, independently of the method used. Apart from the method described below, one could start optimizing from the cuts of a higher or lower mass or energy region. However, this would induce a correlation between

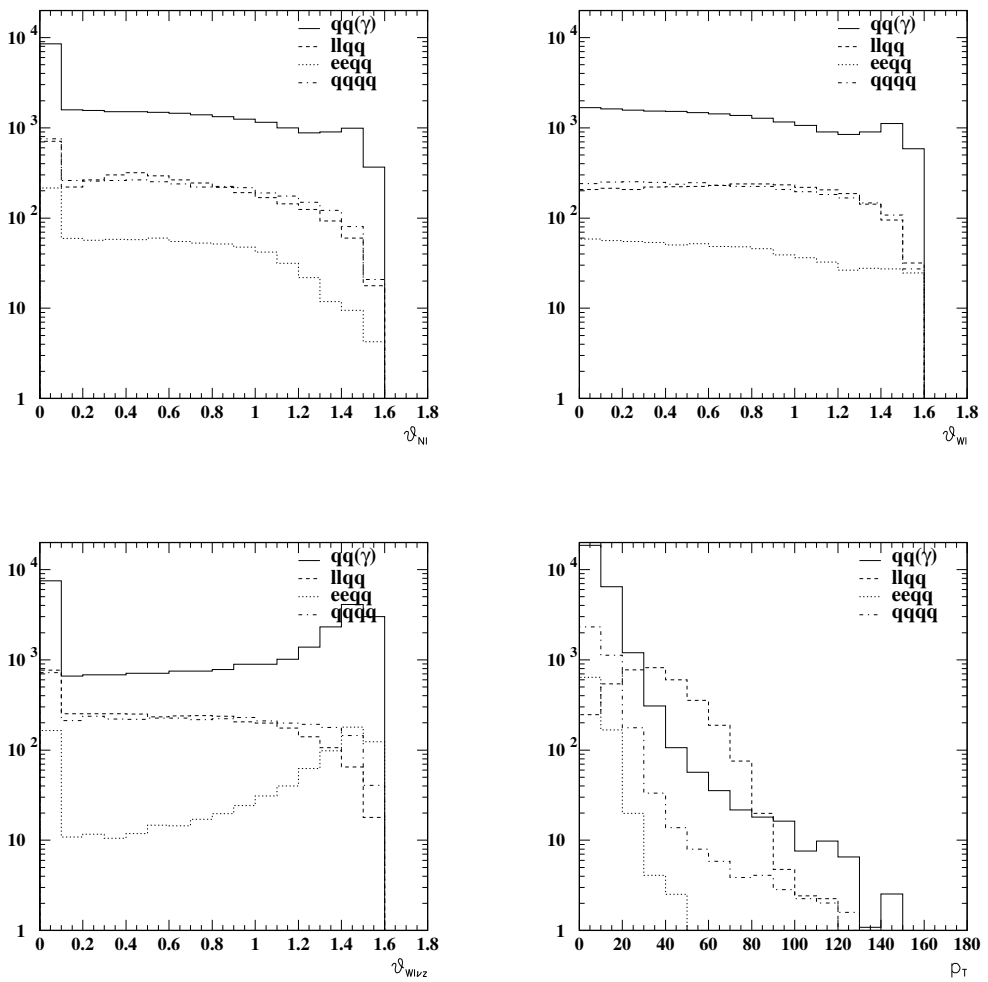

Figure 3-3: Comparison of variables relevant for exotic neutral lepton production for different backgrounds

different masses and energy regions, which is not necessarily real.

Due to the kinematics of the different masses it is not possible to make good mass independent cuts. However, it is possible to make cuts that are functions of the mass (see tables 3-V–3-VII). For an explanation of the different variables, cf. section 3.4.1.

The optimization of cuts has been made in three steps, starting from some very loose general cuts: $5 < E_\ell < 100$, $10 < E_\nu < 100$, $|\cos\theta_{mis}| < 0.95$, $5 < M_{\ell\nu} < 70$.

The first step is a visual estimation of appropriate cuts for the variables M_N, E_ℓ, E_ν, $|\cos\theta_{mis}|$, θ_{Wl}, $\theta_{Wl\nu}(\hat{z})$, and $M_{\ell\nu}$.

At this point, every cut is slightly altered (± 5 GeV or ± 0.1 radians), and those changes are kept, which improve $S/\sqrt{B}$, without too much decreasing the signal. The alteration is then repeated, until no more significant improvements are achieved. This step is done automatically, and because of this a rather high improvement (in the order of several percent) is required to continue. Note that in some cases this optimization implies a broadening of the general cuts.

The last step is a manual fine-tuning of the cuts with the aim of having a high $S/\sqrt{B}$, but still a with signal larger than one. In the evaluation, $S^{3/2}/\sqrt{B}$ is also considered in order to promote high signal cuts. Finally, we require that the decay lepton from the N should be an electron, which cuts none of the real signal (supposing that the heavy lepton is of E-type without any mixing to the μ or τ) but should cut more than half of the background.

a. Statistical Error

The last step in the optimization procedure is somewhat arbitrary in the choice between keeping a lot of signal events and obtaining a high $S/\sqrt{B}$. This is remedied by evaluating the results as they change by varying the cuts (± 2.5 GeV or ± 0.05 radians) and observe the changes. More about this in the next chapter.

b. Comments

The E_ℓ is very low for low masses, while E_ν is high for low masses. θ_{Wl} also increases with the mass. Generally, the widths of the distributions grow with the mass. In the end of the fine-tuning, the cut on the θ_{Nl} turns out to be superfluous. The cuts are summarized in tables 3-V–3-VII.

The principal variables and their cuts are plotted below. Two cases have been chosen, $M_N = 100$ GeV and $M_N = 170$ GeV, both for the center of mass energy range of 191-200 GeV. Everything outside the region marked by the arrows is cut away. As the cuts depend on order, each cut is shown with the other cuts already applied. Note that the binning sometimes is too small, giving the illusion of an excess in the data. Furthermore, the Monte Carlo simulation are often less than one while data obviously is integral. This will also produce the impression that the data does not follow the simulated background.

For each background, the number of remaining events after each consecutive cut is presented in tables 3-VIII and 3-IX. This is useful to see how much a specific background is affected be a certain cut. This could eventually be used to find a different way of optimizing, targeting the most dominant background.

M_N	$\lvert\cos\theta_{\rm vis}\rvert \in$	$M_{\ell\nu} \in$	$E_\nu \in$	$E_\ell \in$	$M_N \in$	$\theta_{W\ell} \in$	$\theta_{W\ell\nu}(\hat{z})\in$
100	$[.15, .9]$	$[15, 73]$	$[60, \infty)$	$[8, 95]$	$[85, 113]$	$[0, .75]$	$[.05, 1.4]$
110	$[.15, .95]$	$[8, 60]$	$[55, 80]$	$[15, 30]$	$[103, 125]$	$[.15, 1.4]$	$[0, 1.55]$
120	$[0, .95]$	$[5, 60]$	$[48, 100]$	$[20, 30]$	$[108, 138]$	$[.5, 1.35]$	
130	$[0, .95]$	$[5, 60]$	$[43, 100]$	$[28, 100]$	$[120, 150]$		$[0, 1.5]$
140	$[0, .95]$	$[8, 63]$	$[38, 65]$	$[28, 50]$	$[133, 158]$	$[.55, 1.5]$	$[0, 1.35]$
150	$[.05, 1]$	$[13, 63]$	$[28, 55]$	$[40, 55]$	$[143, 170]$	$[.95, 1.4]$	$[0, 1.35]$
160	$[.05, .95]$	$[10, 55]$	$[20, 45]$	$[50, 70]$	$[150, 183]$	$[1.1, 1.5]$	$[0, 1.2]$
170	$[0, 1]$	$[18, 65]$	$[10, 30]$	$[55, 78]$	$[158, 188]$	$[1.2, 1.45]$	$[0, 1.3]$

Table 3-V: Summary of cuts for the different masses M_N for the energy region 180-190 GeV. Energies and masses are given in GeV, angles in radians. For explanations of variables, see section 3.4.1. For readability, 2.5 and 7.5 are displayed as 3 and 8, respectively.

M_N	$\lvert\cos\theta_{\rm vis}\rvert \in$	$M_{\ell\nu} \in$	$E_\nu \in$	$E_\ell \in$	$M_N \in$	$\theta_{W\ell} \in$	$\theta_{W\ell\nu}(\hat{z})\in$
100	$[.15, .95]$	$[23, 78]$	$[60, 90]$	$[10, 23]$	$[88, 115]$	$[0, .8]$	$[0, 1.6]$
110	$[.05, .95]$	$[8, 70]$	$[60, 85]$	$[13, 28]$	$[103, 128]$	$[0, 1.35]$	$[0, 1.45]$
120	$[0, .95]$	$[10, 63]$	$[50, 80]$	$[20, 38]$	$[105, 133]$	$[.2, 1.35]$	$[.05, 1.4]$
130	$[0, .95]$	$[13, 73]$	$[50, 78]$	$[25, 40]$	$[120, 150]$	$[.55, 1.35]$	$[.05, 1.2]$
140	$[0, 1]$	$[10, 68]$	$[38, 70]$	$[30, 48]$	$[118, 155]$	$[.7, 1.4]$	$[0, 1.5]$
150	$[0, 1]$	$[8, 85]$	$[35, 58]$	$[38, 53]$	$[138, 168]$	$[.85, 1.5]$	$[0, 1.4]$
160	$[0, .95]$	$[13, 63]$	$[25, 48]$	$[38, 65]$	$[150, 180]$	$[.95, 1.45]$	$[0, 1.05]$
170	$[0, 1]$	$[23, 73]$	$[15, 40]$	$[53, 78]$	$[160, 193]$	$[1.05, 1.4]$	$[0, .95]$

Table 3-VI: Summary of cuts for the different masses M_N for the energy region 191-200 GeV. Energies and masses are given in GeV, angles in radians.

3.6 Discussion of Heavy Charged Leptons

The process we are studying is shown in figure 2-1(a). If the heavy lepton mass is not close to the centre of mass energy ($\sim$ 200 GeV) there will be much energy left for the recoiling lepton ℓ. This energy will be mostly deposited in the beam direction, due

M_N	$\lvert\cos\theta_{\rm vis}\rvert \in$	$M_{\ell\nu} \in$	$E_\nu \in$	$E_\ell \in$	$M_N \in$	$\theta_{W\ell} \in$	$\theta_{W\ell\nu}(\hat{z}) \in$
100	$[.1, .95]$	$[20, 75]$	$[65, 105]$	$[10, 23]$	$[83, 115]$	$[0, .9]$	$[.1, 1.5]$
110	$[0, .95]$	$[10, 73]$	$[63, 95]$	$[13, 28]$	$[100, 128]$	$[0, 1.15]$	$[.05, 1.45]$
120	$[.1, .95]$	$[10, 73]$	$[60, 95]$	$[20, 33]$	$[108, 135]$	$[.2, 1.35]$	$[.05, 1.45]$
130	$[.1, 1]$	$[20, 73]$	$[55, 75]$	$[28, 40]$	$[115, 145]$	$[.45, 1.3]$	$[0, 1.4]$
140	$[.1, .95]$	$[18, 75]$	$[48, 68]$	$[30, 45]$	$[128, 160]$	$[.7, 1.3]$	$[0, 1.5]$
150	$[.45, 1]$	$[25, 123]$	$[43, 58]$	$[38, 73]$	$[135, 163]$	$[.55, 1.3]$	$[0, 1]$
160	$[0, 1]$	$[15, 93]$	$[35, 58]$	$[33, 65]$	$[150, 180]$	$[.85, 1.4]$	$[0, 1.1]$
170	$[.05, 1]$	$[20, 98]$	$[20, 45]$	$[48, 70]$	$[150, 188]$	$[1, 1.4]$	$[0, .95]$

Table 3-VII: Summary of cuts for the different masses M_N for the energy region 201-210 GeV. Energies and masses are given in GeV, angles in radians.

Cut	llqq	qqγ	eeqq	qqqq	ee$\tau\tau$	$\gamma^*\gamma$qq
E_ν	788.30	1546.9	124.10	197.50	1.22	25.23
E_ℓ	126.80	354.5	32.57	3.02	0.10	4.93
$\lvert\cos\theta\rvert$	22.52	126.43	12.58	1.22	0.03	0.73
$M_{\ell\nu}$	17.54	6.59	0.25	0.32	0.01	0
$\theta_{W l\nu}(\hat{z})$	14.22	4.44	0.22	0.19	0.01	0
$\theta_{W l}$	14.22	4.44	0.22	0.19	0.01	0
M_N	9.40	3.13	0.19	0.02	0	0
Type=E	4.08	0.24	0.04	0	0	0

Table 3-VIII: Number of remaining events for different backgrounds before each cut for $M_N = 100$ GeV in the energy region 191-200 GeV.

to spin conservation, making the lepton escape the detector. Consequently, both the lepton and the high-energetic neutrino will be missing, thus making the reconstruction very difficult.

Hence, for heavy leptons, only really high masses are easily detectable. This is illustrated in figure (3-7). The problem with the higher masses is that the cross sections are low (cf. figure 3-8). The low electron energy also causes problems due to the background (see figure 3-3).

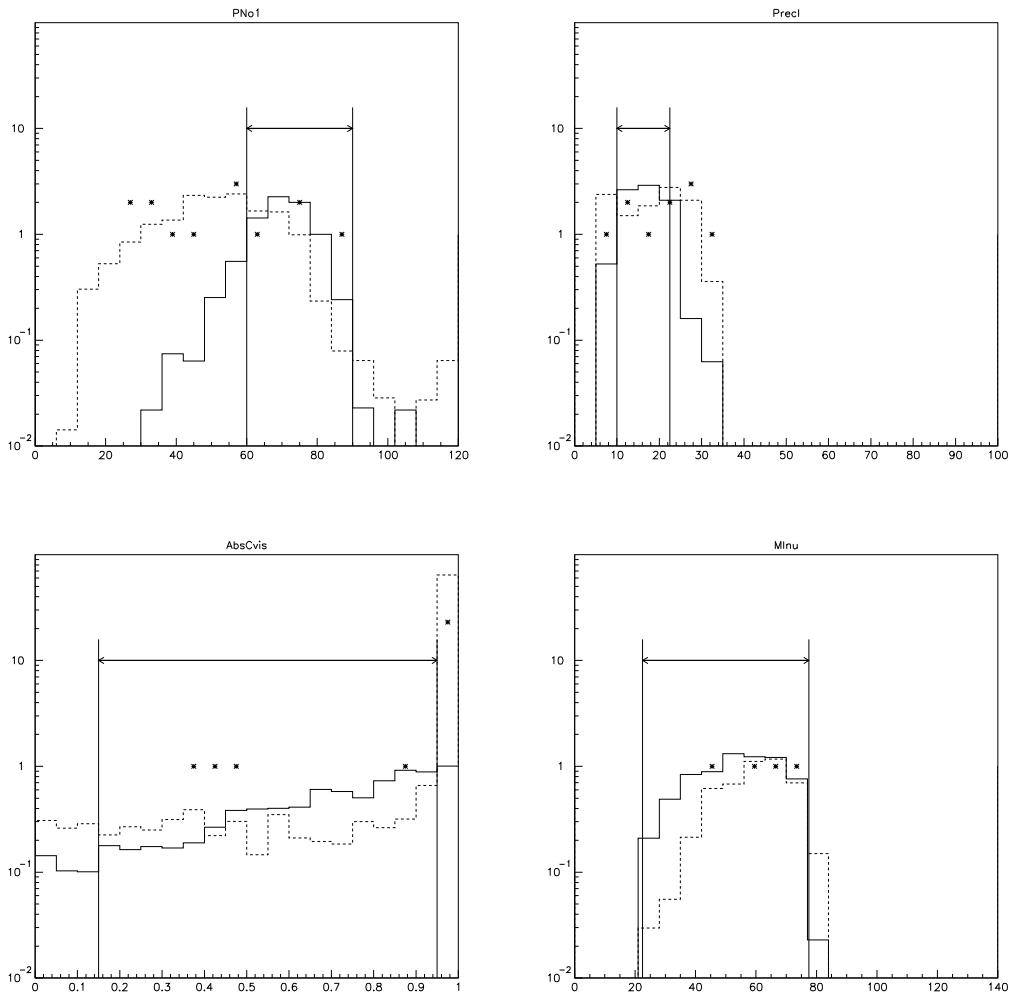

Figure 3-4: Cuts for $M_N = 100$ GeV in the energy region 191-200 GeV. The background (dotted lines) has been plotted for comparison. Data (stars) have been plotted for reference but have not been used in any way during the optimization.

There are two possible approximations which might help to identify and separate the lepton and the neutrino. In the first approximation, we suppose that the $p_T(\nu) >> p_T(\ell) \approx 0$, which could be a good estimate for high masses. In the second approximation we assume that $p_z(\ell) >> p_z(\nu) \approx 0$, which is a good estimate for low masses, when the lepton has much energy and the neutrino has little. Neither of these approximations has been tested yet.

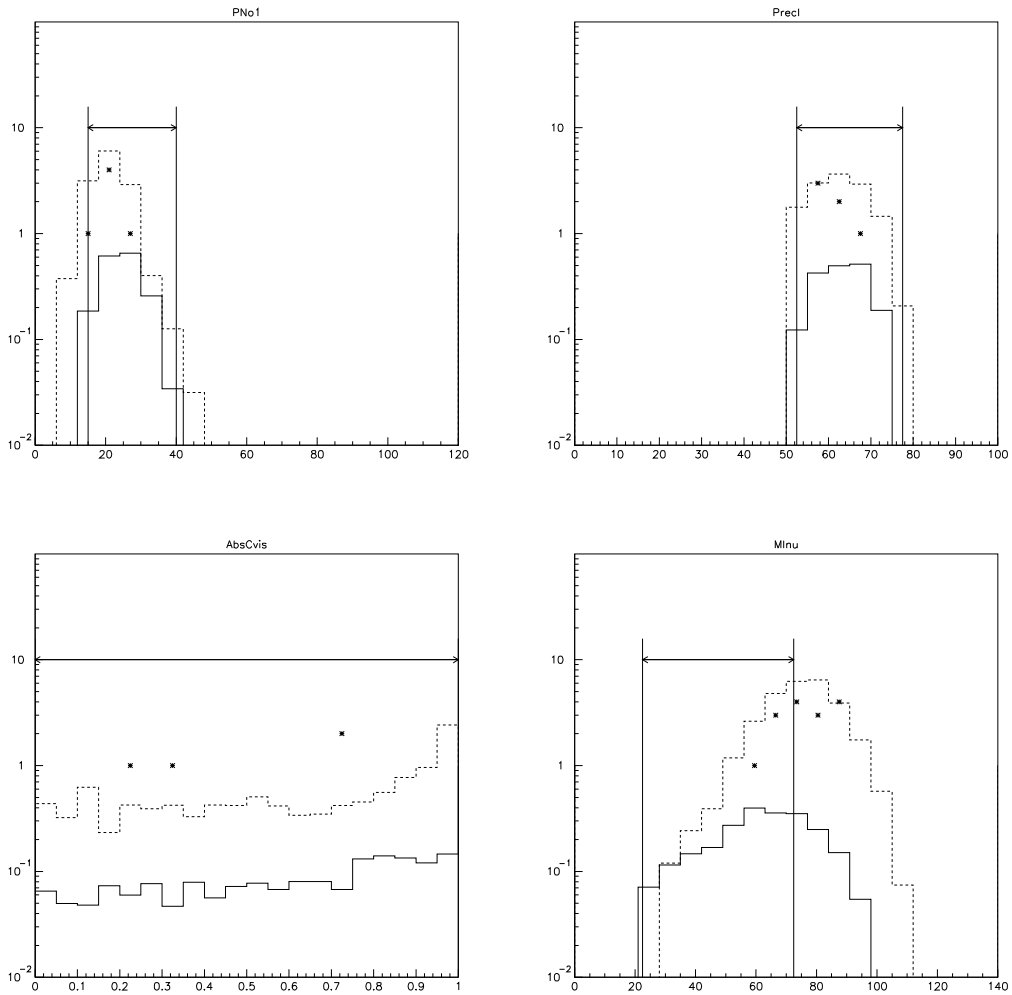

Figure 3-5: Cuts for $M_N = 170$ GeV in the energy region 191-200 GeV. The background (dotted lines) has been plotted for comparison. Data (stars) have been plotted for reference but have not been used in any way during the optimization.

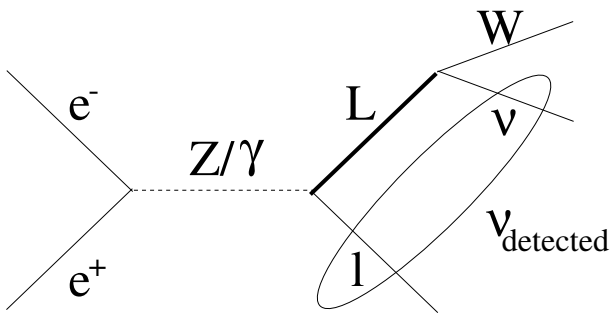

Figure 3-6: When the primary lepton moves very close to the beam pipe, it escapes detection and is confounded with the neutrino.

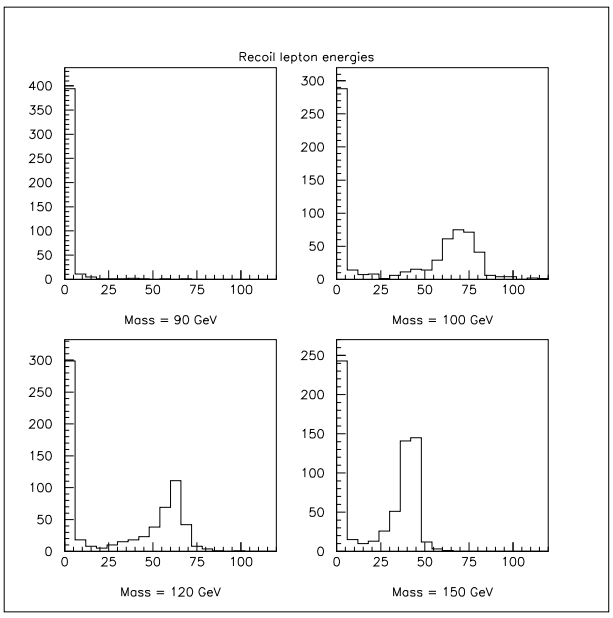

Figure 3-7: Energies of detected recoil leptons for M_L =90, 100, 120, 150 GeV.

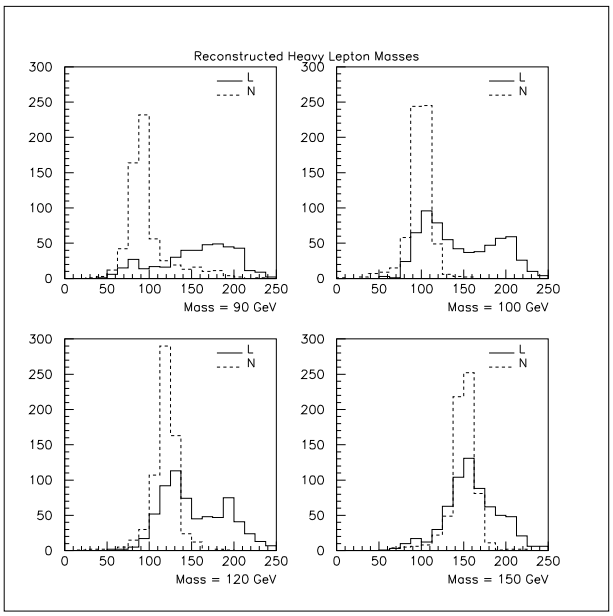

Figure 3-8: Pre-detector evaluation of signals. Reconstructed heavy charged lepton (L) mass for M =90, 100, 120, 150 GeV. The corresponding heavy neutral lepton (N) reconstructed mass in included for reference (dotted lines). We note that the lower energy has a very bad resolution in the charged lepton case.

Cut	llqq	qqγ	eeqq	qqqq	ee$\tau\tau$	$\gamma^*\gamma$qq
E_ν	788.30	1546.9	124.10	197.50	1.22	25.23
E_ℓ	321.30	498.7	34.33	79.34	0.53	8.09
$\lvert\cos\theta\rvert$	166.50	7.29	6.32	0.17	0.08	1.50
$M_{\ell\nu}$	166.50	7.29	6.32	0.17	0.08	1.50
$\theta_{Wl\nu}(\hat{z})$	45.22	3.45	4.12	0.01	0.07	0.18
θ_{Wl}	34.11	2.8	3.34	0.01	0.07	0.18
M_N	16.52	1.09	1.72	0	0.01	0.18
Type=E	7.15	1.08	1.72	0	0.01	0.18

Table 3-IX: Number of remaining events for different backgrounds before each cut for $M_N = 170$ GeV in the energy region 191-200 GeV.

Chapter 4

Data Analysis and Results

This chapter contains analysis of the data and the results in the form of limits on the *mixing parameter* ζ. The number of measured data-events is referred to as data, D, the simulated background events as B and the simulated signal S. Furthermore, the analysis has been grouped into three energy regions, 183-189 GeV, 192-200 GeV and 202-209 GeV as discussed in chapter 3.

4.1 Heavy Neutral Lepton

Limits have been set on the mixing parameter, ζ, rather than on the production cross sections because the mixing parameter is constant for all mass regions. The limits on the cross sections will be different for every mass and center of mass energy. These limits can be obtained by the use of the values in table 2-I along with the limits on ζ^2 in tables 4-III to 4-V below. The cross section, σ is proportional to the square of the mixing parameter: $\sigma \propto \zeta^2$.

- For more than 15 background events or more than 20 data events, the limit is extracted with the assumption of gaussian statistics. We look at a single-sided gaussian distribution so that a 95% confidence limit corresponds to $1.64\bar{\sigma}$ (like a 90% double-sided limit), where the standard deviation, $\bar{\sigma} = \sqrt{B + S_{95}}$, B is the background, S_{95} is the signal with a mixing required to obtain this confidence

level (see figure 4-1).

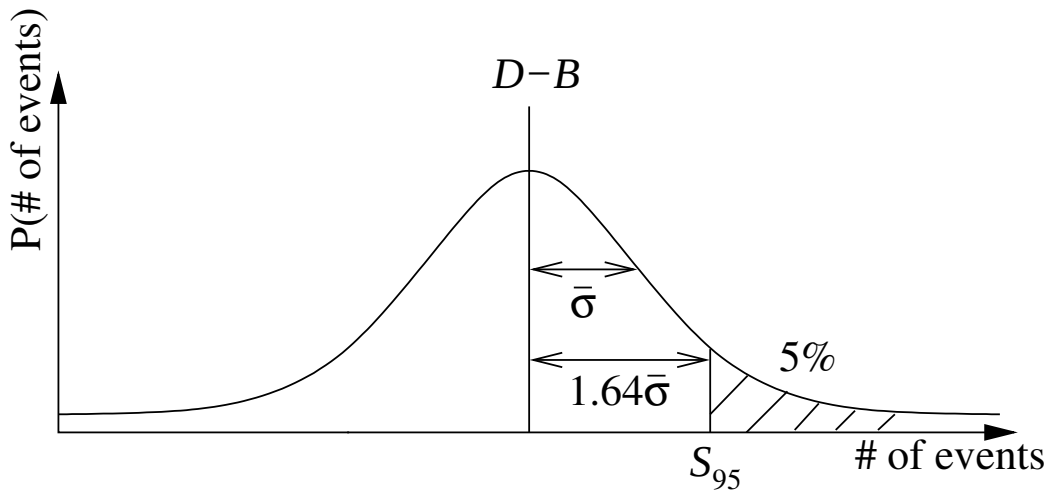

Figure 4-1: Illustration of the statistic distribution

Thus, with 95% C.L., we solve the equation

$$1.64\bar{\sigma} = S_{95} - (D - B), \tag{4.1}$$

for S_{95} (D is the measured number of data-events). The number of data-events is proportional to the cross section which is proportional to the squared mixing angle, hence we obtain an upper limit on the mixing angle with 95% confidence level: $\zeta^2(95\%) = S_{95} * \zeta^2/S$ where S is the simulated signal and ζ^2 is the square of the nominal mixing (see section 3.2.2).

- For small data and/or backgrounds the gaussian approximation is no longer valid, and the method in [60] has been used to determine the limits. In the article, there are tables for different confidence limits, data, and expected background.

The number of signal, background, and data events, preceeding each consecutive cut, is shown in tables 4-I and 4-II. The tables show two representative cases, $M_N =$ 100 GeV and $M_N = 170$ GeV, both in the 191-200 GeV energy region.

In the $M_N = 100$ GeV case (table 4-I), we note that the cut on the polar angle seems to reduce the $S/\sqrt{B}$, but this is because the result is order-dependent (as discussed in section 3.5.1). The final result (Type=E) has a better $S/\sqrt{B}$ with the $|\cos\theta|$ cut than without it. In this case, the cut on $\theta_{Wl\nu}(\hat{z})$ proves to be useless, which can easily be understood in the light of table 3-VI where we see that there is no cut on this variable for this mass. The background corresponds pretty well to the data all along.

In the $M_N = 170$ GeV case (table 4-II), we note that the $S/\sqrt{B}$ never even gets close to that of $M_N = 100$ GeV. One of the reasons for this is the lower cross section (because of its mass), another reason is the persistence of the llqq background (see table 3-IX) caused by the similarity of the lepton and neutrino energy for the signal and the llqq background (see 3-5 and 3-1). In this case, the $M_{\ell\nu}$ cut turns out to be unecessary, though it is still included for completeness.

Cut	$S/\sqrt{B}$	Data	Bg	Signal
E_ν	0.46	2674	2683.0	24.1
E_ℓ	0.83	518	522.0	19.0
$\|\cos\theta\|$	0.76	146	163.5	9.7
$M_{\ell\nu}$	1.64	22	24.7	8.2
$\theta_{Wl\nu}(\hat{z})$	1.81	15	19.1	7.9
θ_{Wl}	1.81	15	19.1	7.9
M_N	2.08	9	12.8	7.4
Type=E	3.33	4	4.4	6.9

Table 4-I: Number of remaining events before each cut for $M_N = 100$ GeV in the energy region 191-200 GeV.

4.1.1 Lower Limits on the Mixing

In the first attempt to analyse the data, there were considerably more data left, after the cuts, than expected. This excess called for a more thorough analysis, which, how-

Cut	$S/\sqrt{B}$	Data	Bg	Signal
E_ν	0.11	2674	2683.0	5.5
E_ℓ	0.15	969	942.3	4.7
$\lvert\cos\theta\rvert$	0.26	150	181.9	3.5
$M_{\ell\nu}$	0.26	150	181.9	3.5
$\theta_{Wl\nu}(\hat{z})$	0.30	32	53.1	2.2
θ_{Wl}	0.32	24	40.5	2.0
M_N	0.38	13	19.5	1.7
Type=E	0.52	5	10.1	1.7

Table 4-II: Number of remaining events before each cut for $M_N = 170$ GeV in the energy region 191-200 GeV.

ever, did not confirm the excess. There are still a couple of masses around $M_N \sim$140 GeV, which have an excess, but considering that there are 24 results, this is not considered significant.

Just before applying the last cut (requiring that the lepton should be an electron) there is a noticeable excess in the data for certain points in the $(M_N, \sqrt{\hat{s}})$-plane. In these cases we can also calculate lower limits on the mixing. In the energy region 180-190 GeV there is one lower limit with 99% CL at M_N =120 GeV, two lower limits with 90% CL at M_N=100 and 130 GeV, and one lower limit with 68% CL at M_N =160 GeV. This means that the probability of *not* having a new particle is less than 1% for $(M_N, \sqrt{\hat{s}}) = (120, 180-190)$. However, the total number of events remaining after all cuts is too small to allow any definite conclusions. Furthermore, in the energy region 191-200 GeV, there is a lower limit with 95% for M_N=140 GeV and a lower limit with 68% CL at M_N=150 GeV. Finally, in the energy region 201-208 GeV, there are two lower limit with 68% CL at M_N=120 and 130 GeV. This seems to indicate that something special is going on at $M_N \sim 130$ GeV. Nevertheless, it is peculiar that this excess only appears before the final cut. After that cut, the excess disappears and the data corresponds well to the expected background. The signal we are looking for requires the lepton to be of electron type. Hence, the observed excess doesn't come from the expected process. However, if the lepton is of muon type it could possibly

give this result. This is definitely something that is worth to investigate further.

Nevertheless, the excess is not detected in all the energy regions, thus weakening the probability of the excess to be a real signal.

4.1.2 Upper Mixing Limits

The upper limits on the mixing between ordinary and heavy leptons for each energy region is presented in tables 4-III to 4-V. We note that in most cases, the data and the expected background correspond very well.

Furthermore, table 4-VI shows the combination of the three energy regions. The combination has been obtained like

$$1/\zeta^2 = \sum_{i=energyregions} 1/\zeta_i^2.$$

If $\zeta_i = 0$ it has been ignored, nothing can be concluded from this. For certain masses, the upper limits are improved with respect to the estimated 0.005 [36, 37]. The reason for the higher limits for masses $\sim$ 130 GeV is a certain excess in the data (compare with section 4.1.1). It is also noteworthy that the statistics are rather low and the results should therefore be regarded with certain caution.

4.1.3 Systematic Errors

There are several types of systematic errors: theoretical, simulation, normalization and reconstruction. These errors are presented below.

M_N	Data	Bg	Signal	$1000 * \zeta^2(95\%)$
100	5	2.7	7.7	5.49
110	1	0.7	3.5	6.20
120	0	0.3	2.9	0.00
130	0	0.5	2.7	0.00
140	0	0.6	2.5	0.00
150	1	1.2	2.0	9.67
160	1	0.6	1.6	13.25
170	6	6.6	1.9	16.78

Table 4-III: Upper limits on the mixing parameter, ζ^2, with 95% CL, for different masses and in the energy region 180-190 GeV. Note that the values given for the mixing parameter have to be divided by 1000.

M_N	Data	Bg	Signal	$1000 * \zeta^2(95\%)$
100	4	4.0	7.2	3.36
110	4	3.3	3.5	9.37
120	1	1.3	2.5	7.92
130	0	0.2	1.8	0.00
140	2	2.7	2.3	8.70
150	2	1.5	1.4	16.86
160	1	1.2	1.3	14.88
170	5	9.3	1.7	8.83

Table 4-IV: Upper limits on the mixing parameter, ζ^2, with 95% CL, for different masses and in the energy region 191-200 GeV. Note that the values given for the mixing parameter have to be divided by 1000.

M_N	Data	Bg	Signal	$1000 * \zeta^2(95\%) <$
100	5	7.2	8.9	2.21
110	5	7.0	6.0	3.16
120	3	1.7	2.4	13.44
130	3	1.3	2.4	14.69
140	0	0.6	1.7	0.00
150	20	17.4	3.6	15.84
160	12	16.7	3.2	3.88
170	28	31.7	3.2	10.04

Table 4-V: Upper limits on the mixing parameter, ζ^2, with 95% CL, for different masses and in the energy region 201-208 GeV. Note that the values given for the mixing parameter have to be divided by 1000.

M_N	100	110	120	130	140	150	160	170
$1000 * \zeta^2(90\%CL) <$	0.79	1.27	4.12	12.96	6.97	3.58	0.84	2.46
$1000 * \zeta^2(95\%CL) <$	1.07	1.71	4.98	14.69	8.70	4.43	2.50	3.67

Table 4-VI: Combined upper limits on the mixing parameter for different masses for the the three energy regions. The nominal value of the mixing parameter is $\zeta^2 = 0.005$.

a. Theoretical

- Intergenerational mixing could exist.
- Extra light gauge bosons (e. g. Z') could affect an eventual signal.

b. Simulation

- The simulation of the backgrounds is inexact, especially the hadronization.
- More background simulations for $E_{CMS} = 189$ GeV could help as discussed in section 3.3.
- The GOPAL detector simulator is not exactly correct.

c. Normalization

- Luminosities could be somewhat different.

d. Reconstruction

- The reconstruction of leptons is not perfect.
- The use of energy regions instead of optimizing the cuts individually for every energy. This can be particularly important for high masses in the center of mass energy region 180-190 GeV.
- Problems with the detector (e. g. calibration).

The number of events before cuts is very similar for the background and the data (see table 4-I), which means that the background is well simulated. The signal would be

far too small to be seen without any cuts.

In tables 4-VII and 4-VIII, the sensitivity of the cuts is shown. The first table presents $M_N = 100$ GeV and the second $M_N = 170$ GeV, both in the 191-200 GeV energy region. Every cut has been changed individually, modifying the cut ± 2.5 GeV (or ± 0.1 for angles). As we can see, there is no major change in the results ($S/\sqrt{B}$). We note that the $|\cos\theta|$ cut in the $M_N = 100$ GeV case is very significant. This is quite normal considering the form of the background for this variable (see figure 3-1). The low mass does not allow for an agressive cut on the lepton energy. This results in leptons close to the beam-pipe, i. e. leptons with $|\cos\theta| \sim 1$. However, when $|\cos\theta|$ is very close to 1, the leptons escape the detector (see section 1.6).

Variable	$S/\sqrt{B}$	Data	Bg	Signal
$57.5<E_\nu<90$	3.45	7	5.0	7.7
$62.5<E_\nu<90$	3.60	3	3.4	6.6
$60<E_\nu<92.5$	3.58	4	4.0	7.2
$60<E_\nu<87.5$	3.58	4	4.0	7.2
$12.5<E_\ell<22.5$	3.27	3	3.5	6.1
$7.5<E_\ell<22.5$	3.30	4	5.0	7.4
$10<E_\ell<20$	3.48	3	2.9	5.9
$10<E_\ell<25$	3.38	5	5.5	8.0
$0.1<\lvert\cos\theta\rvert<0.95$	3.54	4	4.3	7.4
$0.2<\lvert\cos\theta\rvert<0.95$	3.60	4	3.8	7.0
$0.15<\lvert\cos\theta\rvert<1$	1.29	27	40.5	8.2
$0.15<\lvert\cos\theta\rvert<0.9$	3.39	4	3.5	6.4
$25<M_{\ell\nu}<77.5$	3.54	4	4.0	7.1
$20<M_{\ell\nu}<77.5$	3.58	4	4.0	7.2
$22.5<M_{\ell\nu}<75$	3.59	4	3.9	7.1
$22.5<M_{\ell\nu}<80$	3.56	4	4.1	7.2
$0.05<\theta_{Wl}<0.8$	3.31	4	3.9	6.6
$0<\theta_{Wl}<0.85$	3.50	4	4.4	7.3
$0<\theta_{Wl}<0.75$	3.63	4	3.8	7.0
$0.05<\theta_{Wl\nu}(\hat{z})<1.6$	3.59	4	3.9	7.1
$0<\theta_{Wl\nu}(\hat{z})<1.55$	3.57	4	4.0	7.2
$0<\theta_{Wl\nu}(\hat{z})<1.65$	3.58	4	4.0	7.2
$85<M_N<115$	3.52	4	4.3	7.3
$90<M_N<115$	3.39	4	3.9	6.7
$87.5<M_N<117.5$	3.49	4	4.3	7.2
$87.5<M_N<112.5$	3.66	2	3.6	7.0

Table 4-VII: Effect on the results for changes in cuts for $M_N = 100$ GeV in the center of mass energy region 191-200 GeV

Variable	$S/\sqrt{B}$	Data	Bg	Signal
$12.5<E_\nu<40$	0.55	6	10.4	1.8
$17.5<E_\nu<40$	0.53	5	8.2	1.5
$15<E_\nu<42.5$	0.56	5	9.3	1.7
$15<E_\nu<37.5$	0.55	5	9.3	1.7
$55<E_\ell<77.5$	0.55	5	8.1	1.6
$50<E_\ell<77.5$	0.56	5	10.1	1.8
$52.5<E_\ell<75$	0.55	5	9.3	1.7
$52.5<E_\ell<80$	0.56	5	9.5	1.7
$0.05<\lvert\cos\theta\rvert<1$	0.54	4	9.1	1.6
$0<\lvert\cos\theta\rvert<1.05$	0.55	5	9.3	1.7
$0<\lvert\cos\theta\rvert<0.95$	0.56	5	7.7	1.6
$25<M_{\ell\nu}<72.5$	0.54	5	9.3	1.6
$20<M_{\ell\nu}<72.5$	0.56	5	9.3	1.7
$22.5<M_{\ell\nu}<70$	0.57	4	7.7	1.6
$22.5<M_{\ell\nu}<75$	0.53	6	11.3	1.8
$1<\theta_{Wl}<1.4$	0.54	5	9.9	1.7
$1.1<\theta_{Wl}<1.4$	0.57	4	8.5	1.7
$1.05<\theta_{Wl}<1.45$	0.53	5	10.3	1.7
$1.05<\theta_{Wl}<1.35$	0.53	5	8.2	1.5
$0.05<\theta_{Wl\nu}(\hat{z})<0.95$	0.52	5	8.8	1.5
$0<\theta_{Wl\nu}(\hat{z})<0.9$	0.56	5	8.9	1.7
$0<\theta_{Wl\nu}(\hat{z})<1$	0.56	5	9.7	1.7
$157.5<M_N<192.5$	0.56	5	9.8	1.7
$162.5<M_N<192.5$	0.55	5	8.6	1.6
$160<M_N<195$	0.55	5	9.4	1.7
$160<M_N<190$	0.55	5	9.1	1.7

Table 4-VIII: Effect on the results for changes in cuts for $M_N = 170$ GeV in the center of mass energy region 191-200 GeV.

Chapter 5

Conclusions and Outlook

5.1 Conclusions

This is a search for heavy neutrinos in the single production channel with charged current decay, which gives two jets ($e^+e^- \to N\nu \to W\ell\nu \to 2\,\text{jets}+\ell\nu$). No traces of additional neutrinos have been found, which is quantified by new limits on the mixing parameter, established for different masses (see table 4-VI). Masses between 100 and 170 GeV have been analysed at intervals of 10 GeV. The search has been done on OPAL data in the energy region 180-209 GeV with a total integrated luminosity of 663 pb^{-1}. The data has been divided in three energy regions, 180-190 GeV, 191-200 GeV, and 201-208 GeV. Main as well as minor backgrounds have been considered and every energy region and mass has been individually optimized.

5.2 Outlook

In order to complete the analysis, it would be interesting to investigate the neutral current channel as well as heavy charged leptons. For the heavy charged leptons, an approximation has to be made (see section 3.6) and it would be important to evaluate its validity and/or look for other options. The neutral current channel has a lower branching ratio than the charged current channel, but for high masses it could still be a competitive complement.

The peculiar excess in the data just before the last cut is also something that is worth investigating. This could be a signal of a heavy muon even though the number of measured data-events is low. Even though the optimization would be different, there are many common points between a heavy muon and a heavy electron and the cuts could be rather similar for the two cases. However, for the muon it would be an s-channel process, which has a lower cross section.

Furthermore, the cuts can be optimized differently. The fine-tuning described in section 3.5.1 has not necessarily been pushed to its limit. Some cuts could be harder for some mass cases and loser for others. It would also be possible to do a likelihood analysis. This could be a good method of analysis considering the many cuts and the fact that several of them are interdependent.

Appendix A

Glossary

Antimatter Antimatter is constituted of *antiparticles*.

Antiparticle An antiparticle is defined as having the opposite *quantum numbers* of the corresponding particle, but the same mass. Particles with their quantum numbers zero, except for spin which should be integer, (like the photon) are their own antiparticles.

Branching ratio The relative probability that a particle will decay in a specific way. Example: $Z^0 \to e^+e^-$ has a branching ratio of about 3 percent. The sum of all branching ratios should be unity.

Charge conjugation(C) C is an operation that reverses the charge of a particle.

Charged Current (CC) Charged current is an interaction via a W boson.

CP-violation The violation of the charge (C) and parity (P) quantum numbers.

CKM-matrix The mixing between quarks.

Decay channels The possible decays of a particle.
Example:

$$Z^0 \to u\bar{u}, d\bar{d}, s\bar{s}, c\bar{c}, b\bar{b}, t\bar{t}, e^-e^+, \mu^-\mu^+, \tau^-\tau^+, \nu_e\bar{\nu}_e, \nu_\mu\bar{\nu}_\mu, \nu_\tau\bar{\nu}_\tau,$$

where the different processes have different *branching ratios*.

Exotic An exotic particle is either heavy or excited.

Fermion A fermion is a lepton or a quark.

Final state radiation Final state radiation is decays of particles or emission of gluons or photons that occur after the event.

Higgs boson A hypothetical particle required in the standard model of particle physics. The Higgs boson explains why $W^{\pm}$, and Z^0 have a mass.

Initial state radiation Initial state radiation is decays of particles or emission of gluons or photons that occur before the event.

Preons Preons are the consituents of leptons and/or quarks.

Indices L and R These indices refer to left-handed and right-handed particles (for left-handed particles the spin is antiparallell with the direction of the particle, the spin points "backwards").

Massshell On the mass shell means that the particle is real ($M^2 = E^2 - |\vec{p}|^2$). Off the mass shell means that it is virtual ($M^2 \neq E^2 - |\vec{p}|^2$).

Mixing/Mixing parameter/Mixing Angle The mixing between a heavy lepton and an ordinary lepton. For further explanation, see section 1.5.1.

Neutral Current (NC) Neutral current is an interaction via a Z boson.

Parity (P) Parity is an operation that gives a particle the same properties as if is was observed in a "point-like mirror". In other words, the spin of the particle will be inversed. $P\,|parity = p\rangle = |parity = -p\rangle$. The left-parity operator is represented by $P_L = \frac{1}{2}(1 - \gamma_5)$, where γ_5 is defined in appendix B. The right-parity operator is defined as $P_R = \frac{1}{2}(1 + \gamma_5)$.

Signal The signal is the signal of the exotic lepton.

Symmetry A symmetry operation does not change the physical solution. For example, the position of the origin in the coordinate system does not change the physical solution to problem.

***s*-channel** The s-channel is the merging of two particles into one, e. g. $e^+e^- \rightarrow \gamma^*$ (see figure 2-1).

t-channel The t-channel is the exchange of one particle between two other (see figure 2-4).

Quantum numbers The numbers that can be said to best describe the state of a particle. Examples: electric charge (Q), lepton number (L), baryon number (B), parity (P), spin (S), isospin (I), strangeness (S), and charge conjugation (C).

Appendix B

List of Symbols

Regarding the notations used, a capital letter in fermion names signifies a heavy fermion (e. g. L=heavy lepton, E=heavy electron) while a star signifies an excited fermion (e. g. u^*=excited up-quark, μ^*=excited muon). A fermion is either a lepton or a quark, and an exotic particle is either heavy or excited. A lepton L can be either charged or neutral. In both cases a $\pm$ denotes a charged fermion (e. g. $L^{\pm}$=charged heavy lepton). A bar denotes an anti-particle and unless otherwise specified, $c = \hbar = 1$.

B.1 Exotic Particles

F^*	Exotic fermion
L^*	Exotic lepton
F	Heavy fermion
L	Heavy lepton
$L^\pm$	Heavy charged lepton
N	Heavy neutral lepton (neutrino)
E	Heavy electron
N_E	Heavy electron neutrino
Q	Heavy quark
U	Heavy up-quark
D	Heavy down-quark
l^*, ℓ^*	Excited lepton
$l^{*\pm}, \ell^{*\pm}$	Excited charged lepton
ν^*	Excited neutrino
e^*	Excited electron
ν_e^*	Excited electron neutrino
μ^*	Excited muon
ν_μ^*	Excited muon neutrino
τ^*	Excited tau
ν_τ^*	Excited tau neutrino

B.2 Standard Model Particles

γ	Photon
f	Fermion (quark or lepton, origin: Enrico Fermi)
l, ℓ	Lepton (origin: greek leptos=small)
e	Electron (origin: greek elektron = amber, the rubbing of which causes electrostatic phenomena)
ν_e	Electron neutrino (origin: latin "small neutron")
μ	Muon
ν_μ	Muon neutrino
τ	Tauon
ν_τ	Tau neutrino
q	Quark (origin: "Three quarks for Muster Mark" in James Joyce's Finnegans Wake (1939))
u	Up quark
d	Down quark
s	Strange quark
c	Charm quark
t	Top quark
b	Bottom quark
jet	Jet of particles, produced by a quark or a gluon

B.3 Variables

p	Momentum
p_T	Transverse momentum, $p_T \equiv \sqrt{p_x^2 + p_y^2}$ if z is the beam direction
$\mathcal{L}$	Luminosity
σ	Cross-section
θ	Polar angle
ϕ	Azimuthal angle
t	Time
$\bar{\sigma}$	Standard deviation
i	Imaginary number, defined as $i^2 = -1$
γ matrices	$\gamma_0 = \begin{bmatrix} 1 & 0 & 0 & 0 \\ 0 & 1 & 0 & 0 \\ 0 & 0 & -1 & 0 \\ 0 & 0 & 0 & -1 \end{bmatrix}$ $\gamma_5 = \begin{bmatrix} 0 & 0 & 1 & 0 \\ 0 & 0 & 0 & 1 \\ 1 & 0 & 0 & 0 \\ 0 & 1 & 0 & 0 \end{bmatrix}$
	$\gamma_1 = \begin{bmatrix} 0 & 0 & 0 & 1 \\ 0 & 0 & 1 & 0 \\ 0 & -1 & 0 & 0 \\ -1 & 0 & 0 & 0 \end{bmatrix}$ $\gamma_2 = \begin{bmatrix} 0 & 0 & 0 & -i \\ 0 & 0 & i & 0 \\ 0 & i & 0 & 0 \\ -i & 0 & 0 & 0 \end{bmatrix}$ $\gamma_3 = \begin{bmatrix} 0 & 0 & 1 & 0 \\ 0 & 0 & 0 & -1 \\ -1 & 0 & 0 & 0 \\ 0 & 1 & 0 & 0 \end{bmatrix}$

B.4 List of Constants

θ_W	28.7 degrees	The weak mixing angle $\sin^2\theta_W \approx 0.23$
$\hbar$	$1.054571597\times10^{-34}$ Js	$\hbar = h/2\pi$, where h is Planck's constant[1]
c	299792458 ms^{-1}	Speed of light in vacuum[1]
k_B	1.3806503×10^{-23} JK^{-1}	Boltzmann's constant[1]
eV	1.6022×10^{-19} J	Electron Volt

[1] Unless otherwise specified, we set $\hbar = c = k_B = 1$

B.5 Abbreviations

OPAL	Omni-Purpose Apparatus at LEP
CERN	European Laboratory For Particle Physics
	(earlier: Conseil Européen pour la Recherche Nucléaire)
LEP	Large Electron Positron collider
MSSM	Minimal Supersymmetric Standard Model
GUT	Grand Unified Theory
PYTHIA	A FORTRAN program to simulate collisions between particles
grc4f	GRC (Grace) four fermions
kk2f	KK two fermions
QCD	Quantum ChromoDynamics, the field theory for strong interactions
QED	Quantum ElectroDynamics, the field theory for electromagnetic interactions
SUSY	SUper SYmmetry

Bibliography

[1] S.L. Glashow, Nucl. Phys. **22** (1961) 579;
S. Weinberg, Phys. Rev. Lett. **19** (1967) 1264;
A. Salam, *Elementary Particle Theory*, ed. N. Svartholm (Almquist and Wiksells, Stockholm, 1968), 367.

[2] I.A. D'Souza, and C.S. Kalman, *Preons* (Singapore, World Scientific 1992).

[3] J.-J. Dugne, S. Fredriksson, J. Hansson, and E. Predazzi, Proceedings of Beyond 99, Tegernsee, Germany, June (1999).

[4] Q.R. Ahmad et al., *Direct Evidence for Neutrino Flavor Transformation from Neutral-Current Interactions in the Sudbury Neutrino Observatory*, nucl-ex/0204008 (2002).

[5] R.W. Robinett, J.L. Rosner, Phys. Rev. **D 25** (1982) 3036;
P. Langacker, R.W. Robinett, and J.L. Rosner, Phys. Rev. **D 30** (1984) 1470;
V. Barger et al., Phys. Lett. **118 B** (1982) 68.

[6] J. Hewett and T.G. Rizzo, Phys. Rep. **183** (1989) 193.

[7] J. Maalampi and M. Roos, Phys. Rep. **186** (1990) 53.

[8] Q.R. Ahmad et al., Phys. Rev. Lett. **87** (2001) 071301.

[9] M. Gell-Mann, P. Ramond, and R. Slansky, Rev. Mod. Phys. **50** (1978) 721;
T. Yanagida, Phys. Rev. **D 20** (1979) 2986.

[10] ALEPH Collaboration, D. Decamp et al., Phys. Lett. **B 236** (1990) 511;
OPAL Collaboration, M.Z. Akrawy et al., Phys. Lett. **B 240** (1990) 250;
OPAL Collaboration, M.Z. Akrawy et al., Phys. Lett. **B 247** (1990) 448;

L3 Collaboration, B. Adeva et al., Phys. Lett. **B 251** (1990) 321;
DELPHI Collaboration, P. Abreu et al., Phys. Lett. **B 274** (1992) 230.

[11] OPAL Collaboration, G. Alexander et al., Phys. Lett. **B 385** (1996) 433.

[12] L3 Collaboration, M. Acciarri et al., Phys. Lett. **B 377** (1996) 304;
ALEPH Collaboration, D. Buskulic et al., Phys. Lett. **B 384** (1996) 439.

[13] OPAL Collaboration, K. Ackerstaff et al., Phys. Lett. **B 393** (1997) 217.

[14] L 3 Collaboration, M. Acciarri et al., Phys. Lett. **B 412** (1997) 189.

[15] OPAL Collaboration, K. Ackerstaff et al., *Search for Unstable Heavy and Excited Leptons in e+e- Collisions at* $\sqrt(s) = 170 - 172$ *GeV*, Eur. Phys. J. **C 1** (1998) 45.

[16] OPAL Collaboration, K. Ackerstaff et al., Phys. Lett. **B 433** (1998) 195.

[17] DELPHI Collaboration, P. Abreu et al., Eur. Phys. J. **C 8** (1999) 41.

[18] OPAL Collaboration, G. Abbiende et al., Eur. Phys. J. **C 14** (2000), 73.

[19] M. O. de Kok and R. J. Teuscher, *Search for Heavy Charged Leptons and Long-lived Heavy Neutral Leptons*, OPAL Technical Note 706 (2001).

[20] OPAL Collaboration, M.Z. Akrawy et al., Phys. Lett. **B 257** (1990) 531;
ALEPH Collaboration, R Barate et al., Eur. Phys. J. **C 4** (1998) 571;
ALEPH Collaboration, D. Decamp et al., Phys. Lett. **B 250** (1990) 172;
DELPHI Collaboration, P. Abreu et al., Z. Phys. **C 53** (1992) 41;
L 3 Collaboration, M. Acciarri et al., Phys. Lett. **B 353** (1995) 136.

[21] OPAL Collaboration, G. Alexander et al., Phys. Lett. **B 386** (1996) 463.

[22] L 3 Collaboration, M. Acciarri et al., Phys. Lett. **B 370** (1996) 211;
DELPHI Collaboration, P. Abreu et al., Phys. Lett. **B 380** (1996) 480;
ALEPH Collaboration, D. Buskulic et al.,Phys. Lett. **B 385** (1996) 445.

[23] OPAL Collaboration, K. Ackerstaff et al., Phys. Lett. **B 391** (1997) 197.

[24] DELPHI Collaboration, P. Abreu et al., Phys. Lett. **B 393** (1997) 245;
L 3 Collaboration, M. Acciarri et al., Phys. Lett. **B 401** (1997) 139.

[25] L 3 Collaboration, M. Acciarri et al., CERN-EP/99-138, October 1999, accepted by Phys. Lett. B.

[26] H 1 Collaboration, I. Abt et al., Nucl. Phys. **B 396** (1993) 3;
ZEUS Collaboration, M. Derrick et al., Z. Phys. **C 65** (1994) 627;
H 1 Collaboration, S. Aid et al., Nucl. Phys. **B 483** (1997) 44.

[27] OPAL Collaboration, G. Alexander et al., Phys. Lett. **B 377** (1996) 222.

[28] OPAL Collaboration, K. Ackerstaff et al., Phys. Lett. **B 391** (1997) 221;
OPAL Collaboration, K. Ackerstaff et al., Eur. Phys. J. C 2 (1998) 441

[29] The DELPHI OPAL collaborations and the LEP Exotica Working Group, *Search for excited Leptons: LEP combination*, OPAL Technical Note 701 (2001).

[30] M. Gronau, C. N. Leung, and J. L. Rosner, *Extending limits on neutral heavy leptons*, Phys. Rev. **D 29**, 2539 (1984)

[31] *Review of Particle Physics*, D.E. Groom et al.(Particle Data Group), Eur. Phys. J. **C 15** (2000) 1-4, pp. 357

[32] L.M. Johnson, D.W. McKay, and T. Bolton, *Extending sensitivity for low-mass neutral heavy lepton searches* Phys. Rev. **D 56**, (1997) 2970.

[33] H.P. Nilles, Phys. Rep. **110** (1984) 1;
H.E. Haber and G. L. Kane, Phys. Rep. **117** (1985) 75.

[34] J.L. Hewett and T.G. Rizzo, Phys. Rev. **D 56** (1997) 5709.

[35] A. de Rujula, R.C. Giles, and R.L. Jaffe, Phys. Rev. **D 17** (1978) 285;
R. Slansky, T. Goldman, and G.L. Shaw, Phys. Rev. Lett. **47** (1981) 887;
D.G. Caldi and S. Nussimov, Phys. Rev. **D 28** (1983) 3138.

[36] E. Nardi, E. Roulet and D. Tommansini, Phys. Lett. **B 344** (1995) 225.

[37] P. Langacker and D. London, *Mixing between ordinary and exotic fermions*, Phys. Rev. **D 38**, (1988) 886.

[38] T.G. Rizzo, Phys. Rep., *Right-handed currents produced by mixing in E6 theories*, **D 34** (1986) 2076.

[39] ALEPH Coll. Nucl. Instr. Meth. **A 294** (1990) 121;
DELPHI Coll. Nucl. Instr. Meth. **A 303** (1991) 233;
L 3 Coll. Nucl. Instr. Meth. **A 289** (1990) 35;
OPAL Coll. Nucl. Instr. Meth. **A 305** (1991) 275.

[40] The OPAL Detector at LEP, OPAL Collaboration, K. Ahmet et al.Nucl. Instr. Meth. **A 305** (1991) 275.

[41] A. Djouadi, *New fermions at e^+e^- colliders: Production and decay*, Z. Phys. **C 63**, (1994) 317.

[42] R. Tafirout and G. Azuelos, Comp. Phys. Commun. **126** (2000) 244.

[43] OPAL Collaboration, G. Abbiendi et al., *Investigation of single top quark production at $\sqrt{(s)} = 189$ GeV*, OPAL Physics Note 444 (2000).

[44] G. Azuelos, A. Djouadi, *New fermions at e^+e^- colliders: Signals and backgrounds*, Z. Phys. **C 63** (1994) 327.

[45] Comp. Phys. Commun. **66** (1991) 115.

[46] F. Boudjema, A. Djouadi, and J.L. Kneur, Z. Phys. **C 57** 425.

[47] J. Allison et al., Nucl. Instr. Meth. **A 317** (1992) 47;
P. Ward and D. Ward, *A GOPAL Primer*, GOPAL version 1.33 (1995).

[48] T. Sjöstrand, Comp. Phys. Commun. **82** (1994) 74.

[49] T. Sjöstrand, 1994, Comp. Phys. Commun. **82**, 74.

[50] J.H. Kühn, A. Reiter, and P.M. Zerwas, Nucl. Phys. **B 272** (1986) 560.

[51] S. Jadach and J.H. Kuhn, MPI-PAE/Pth 64/86 (1986).

[52] B. Vachon and R. McPherson, *Search for Charged Excited Leptons with Photonic Decay in e+e- Collisions at sqrts=189-202 GeV at LEP*, OPAL Physical Note 434 (2000).

[53] OPAL Coll., S.L. Lloyd, *The OPAL Primer*, Version 98a (1998), 124.

[54] OPAL Collaboration, G. Abbiendi et al., *Search for Single Top Quark Production at LEP2*, Phys. Letts. **B 521** (2001) 181.

[55] S. Jadach, B.F.L. Ward, Z. Was, *The Precision Monte Carlo Event Generator KK For Two-Fermion Final States In e+e- Collisions*, Comp. Phys. Commun. **130** (2000) 260. (hep-ph/9912214.)

[56] R. Engel, Z. Phys. **C 66** (1995) 203;
R. Engel and J. Ranft, Phys. Rev. **64** (1996) 4244.

[57] Y. Kurihara, T. Munehisa, D. Perret-Gallix, Y. Shimizu, and H. Tanaka, *Grc4f v1.1: a four-fermion event generator for e+e- collisions*, Comp. Phys. Commun. **100** (1997) 128

[58] S. Jadach, W. Placzek, M. Skrzypek, B.F. L. Ward, and Z. Was, *Monte Carlo program KoralW 1.42 for all four-fermion final states in e^+e^- collisions* Comp. Phys. Commun. **119** (1999) 272;
S. Jadach et al., Phys. Lett. **B 372** (1996) 289.

[59] ALEPH Coll., G.D. Cowan, *Measurement of α_s from clustered variables in hadronic Z decays*, J. Phys., G, **17** (1991) 1537.

[60] G.F. Feldman and R.D. Cousins, *Phys. Rev.* **D 57** (1998) 3873.

General references

[61] C. Nash, 1978, *Relativistic Quantum Fields*, Academic Press.

[62] M. E. Peskin, D. V. Schroeder, 1995, *An Introduction to Quantum Field Theory*, Addison Wesley Publishing Company.